# *Remote Sensing Estimates of Evapotranspiration from Irrigated Agriculture, Northwestern Nevada and Northeastern California*

**Justin L. Huntington**
**Matthew Bromley**
**Charles G. Morton**
**Timothy Minor**

**December 2018**

**Publication No. 41275**

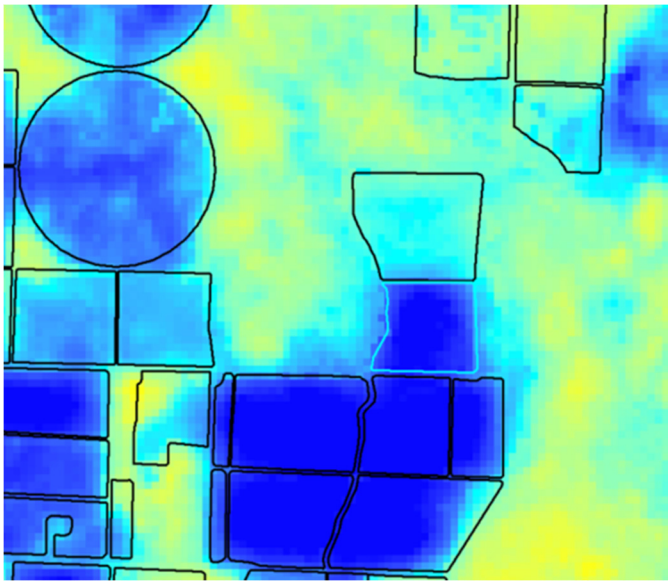

**Prepared by**
Division of Hydrologic Sciences, Desert Research Institute, Reno, NV
Division of Earth and Ecosystem Sciences, Desert Research Institute, Reno, NV

**Prepared for**
U.S. Bureau of Reclamation
Nevada Division of Water Resources

**THIS PAGE INTENTIONALLY LEFT BLANK**

**ABSTRACT**

Accurate historical evapotranspiration (ET) information for agricultural areas in the western U.S. is needed to support crop and pumpage inventories, water right applications, water budgets, and development of water management plans. Annual and monthly ET from irrigated agriculture is largely a function of water availability, atmospheric water demand, crop type, crop conditions, and land use. Landsat thermal and optical satellite imagery is ideal for monitoring the spatial and temporal variability of crops given its spatial and temporal resolution, making it ideal for monitoring crop ET.

The objective of this study is to estimate and summarize monthly, seasonal, and annual ET from agricultural areas in northwestern Nevada and northeastern California from 2001 through 2011 using Landsat satellite imagery. ET estimates from 57 Hydrographic Areas (HAs) are summarized in multiple ways including a geodatabase, maps, figures, and tables. Monthly and annual ET estimates for select HAs are discussed with respect to variations in climate, water supply, and land use changes, through visualizations and summaries of spatial and temporal ET distributions. Landsat based ET was estimated using a land surface energy balance model, Mapping EvapoTranspiration at high Resolution with Internalized Calibration (METRIC), using Landsat 5 and Landsat 7 imagery combined with reference ET. Results highlight that a range of geographic, climatic, hydrographic, and anthropogenic factors influence ET. For example, irrigators in Mason Valley have the ability to mitigate deficiencies in surface water by pumping supplemental groundwater, resulting in low annual ET variability. Conversely, irrigators in Lovelock are subject to limited upstream surface water storage and are not able to irrigate with groundwater due to high salinity. These factors result in high annual ET variability due to drought. ET estimates derived from METRIC for well-watered fields generally compare well to previous estimates derived from traditional reference ET – crop coefficient methods. Although there are limitations and uncertainties with the METRIC model, METRIC ET estimates are within 10 to 20 percent of ET reported from micrometeorological studies in Nevada for commonly grown crops of alfalfa and pasture grass. Landsat derived ET estimates reported in this study have many immediate applications relevant to water managers, researchers, and practitioners.

**THIS PAGE INTENTIONALLY LEFT BLANK**

## CONTENTS

## LIST OF ACRONYMS

| | |
|---|---|
| ASCE-PM | American Society of Civil Engineers standardized Penman-Monteith |
| CLU | Common Land Unit |
| COOP | Cooperative Observer Station |
| ET | Evapotranspiration |
| $ET_{24}$ | 24-hour Evapotranspiration |
| $ET_{inst}$ | Instantaneous Evapotranspiration |
| $ET_r$ | ASCE Standardized Alfalfa Reference Evapotranspiration |
| $ET_{r\_24}$ | 24 hour Reference Evapotranspiration |
| $ET_rF$ | Fraction of Alfalfa Reference Evapotranspiration |
| ETM+ | Enhanced Thematic Mapper Plus |
| G | Ground Heat Flux |
| H | Sensible Heat Flux |
| HA(s) | Hydrographic Area(s) |
| LE | Latent Energy Flux |
| METRIC | Mapping Evapotranspiration at high Resolution with Internalized Calibration |
| NLDAS | National Land Data Assimilation System |
| NWS | National Weather Service |
| PPT | Precipitation |
| PRISM | Parameter Regression on Independent Slopes Model |
| $RH_{max}$ | Daily Maximum Relative Humidity |
| $RH_{min}$ | Daily Minimum Relative Humidity |
| $R_n$ | Net Radiation |
| $R_s$ | Solar Radiation |
| $T_{dew}$ | Dew Point Temperature |
| TM | Thematic Mapper |
| $T_{max}$ | Maximum Air Temperature |
| $T_{min}$ | Minimum Air Temperature |
| u | Wind Speed |
| USGS | United States Geological Survey |
| $\lambda$ | Latent Heat Of Vaporization |
| $\rho$ | Surface Reflectance |

## LIST OF FIGURES

**THIS PAGE INTENTIONALLY LEFT BLANK**

## INTRODUCTION

Reporting of field scale evapotranspiration from irrigated agriculture in the western US states is increasingly being required for surface and groundwater use inventories, development of historical pumpage estimates, and for supporting water right applications and evaluations. The arid landscape of Nevada and California is punctuated by agricultural communities that rely on water supplied by the diversion of surface waters, groundwater, or a combination of both. Like most western U.S. states, the majority of available water is used for irrigated agriculture. Many Hydrographic Areas (HAs) within northwestern Nevada and northeastern California are entirely reliant on groundwater due to the lack of surface water, while other HAs are entirely reliant on surface water due to poor groundwater quality. Precipitation in the form of winter snowfall largely determines the amount of surface water available for irrigation during the growing season. During years of insufficient surface water, many irrigators rely on supplemental groundwater in order to meet irrigation demands.

The arid and yet relatively cool climate of Northern Nevada and California creates conditions optimal for producing high quality dairy and beef hay. Accordingly, alfalfa and grass hay make up the large majority of Nevada's crop acreage, most of which is located in northern Nevada [USDA National Agricultural Statistics Service and Service, 2015]. Due to the large acreage and high water use of hay crops [Jensen et al., 1990], accurate estimates of historical and current water use from hay crops are extremely useful for water management and decision support. For example, the net irrigation water requirement of alfalfa is often used to define the upper limit for a change in the manner of use from irrigation to some other use, such as municipal, environmental, or industrial.

Evapotranspiration (ET) is the combined processes of water lost from the soil surface by evaporation and water lost from plant stomata through transpiration. Several factors affect crop ET, including water availability, crop type, crop phenology, growing season length, management practices, and weather and environmental conditions [Allen et al., 1998; Katerji et al., 1998]. The evaporative demand is largely a function of weather variables such as solar radiation, air temperature, humidity and wind speed. The use of satellite imagery is arguably the only way to accurately estimate ET under actual field conditions over large areas and time periods. Landsat satellite imagery is able to capture field scale conditions, and accurately characterize spatial and temporal variations of crop phenology, stress, management, and therefore ET.

During the past decade, the use of optical and thermal Landsat satellite imagery for estimating crop ET has increased significantly [Anderson et al., 2012; Serbina and Miller, 2014]. This is due, in part, to free access of Landsat imagery as of 2009, coupled with significant advances of ET models, processing hardware, and software. These advances have led applications for mapping ET to the forefront of water management. This is especially true where water consumption from large agricultural areas has to be quantified at field scales for

accurate water accounting. Given that crop ET rates are generally directly proportional to crop yields [Guitjens and Goodrich, 1994], satellite-based monitoring of ET can also provide useful information to growers as to why yields may vary across a field, from field to field, or from year to year. Operational satellite-based crop ET estimation in Nevada will prove extremely useful for water use inventories, developing or reassessing water budgets, crop yield analyses, and for quantifying effects of drought. This report is the basis for ongoing research at the Desert Research Institute focused on operational satellite-based crop ET estimation in Nevada.

## PREVIOUS WORK

Huntington and Allen [2010] estimated daily, monthly, and annual Nevada state-wide crop ET and net irrigation water requirement (NIWR) rates at National Weather Service (NWS) Cooperative Observer (COOP) stations using a reference ET – dual crop coefficient approach. This approach assumes well-watered and stress-free conditions, therefore Huntington and Allen [2010] estimates crop ET and NIWR estimates are representative of potential crop ET rather than the actual crop ET that occurs as a result of spatial and temporal variations in water availability, crop stress and disease, crop management, and water and land use changes. Few studies have estimated field scale crop ET using satellite imagery in northwestern Nevada. While satellite imagery is often used to estimate crop acreage for a limited number of years, crop ET rates are often assumed and applied to respective areas to estimate crop ET volumes. For example, the U.S. Geological Survey (USGS) often assumes that crop ET rates are temporally and spatially constant [Maurer et al., 2006; Allander et al., 2009]. These constant rate ET estimates are then used for developing water budgets [Maurer and Berger, 2006; Lopes and Allander, 2009] and boundary conditions for groundwater models [Halford and Plume, 2011; Yager et al., 2012].

Morton et al. [2013] developed an automated approach for estimating crop ET using a land surface energy balance model applied to Landsat imagery acquired over western Nevada. Morton et al. [2013] compared model based crop ET estimates to ET estimates made at nine eddy covariance and Bowen ratio micrometeorological stations located within irrigated alfalfa and pasture grass fields in Carson Valley and Mason Valley, and reported that mean daily absolute differences between modeled and station based ET ranged from 1 to 27 percent, with the mean absolute difference for all nine sites being approximately 11 percent. In this report, we apply the same Landsat based land surface energy balance model that was outlined in Morton et al. [2013], but with manual calibrations as later described.

## OBJECTIVE

The primary objective of this study is to develop and report field scale estimates of crop ET for irrigated agriculture in northwestern Nevada and north eastern California using Landsat satellite imagery (Figure 1). The study period spans from 2001 through 2011. The secondary objective of the study is to assess field scale seasonal and annual crop ET

estimates for selected HAs of Lovelock, Carson Desert (Fallon), Mason Valley, and Honey Lake Valley (Fish Springs Ranch) with respect to variations in climate, water supply, reference ET, and land use changes, through illustrations of spatial and temporal ET distributions.

## STUDY AREA

The study area is defined by four Landsat scenes, located in northwestern Nevada and parts of northeastern California (Figure 1). The most extensive agricultural areas are located within the hydrographic basins of the Truckee River, Carson River, Walker River, and lower portions of the Humboldt River. The study area includes 57 HAs in total. HAs and respective yearly agricultural field acreages derived in this study are listed in Appendix 1. Climate within the study area is characterized as arid to semi-arid, with mean annual precipitation ranging from 100 to 250 mm within agricultural areas, and approximately 80 percent of precipitation occurring during winter months. The hottest month is July with an average high of 90 °F, and the coldest month is December, with an average low of 15 °F. Agricultural areas are surrounded by rangelands that are mostly composed of phreatophytic and xerophytic shrub species. Alfalfa and grass hay are the principal crops grown within the study area, with marginal amounts of spring and winter grain, corn, potatoes, onions, and garlic [USDA National Agricultural Statistics Service and Service, 2015].

## APPROACH

A land surface energy balance approach is applied for estimating crop ET using model called Mapping EvapoTranspiration at high Resolution with Internalized Calibration (METRIC) [Allen et al., 2007a, 2007b]. Primary model inputs are derived from a combination of optical and thermal Landsat satellite imagery, and agriculturally representative station and gridded weather data. The desired spatial resolution to discriminate agricultural features and perform crop ET calculations so that they are applicable for field scale assessments, is approximately 100 m [Anderson et al., 2012; Yan and Roy, 2016]. Landsat imagery, which was made freely available to the public as of 2009, has a native spatial resolution of 30 m for optical channels and up to 120 m for thermal channels. Landsat imagery is available every 16 days with a single satellite (e.g. Landsat 5 Thematic Mapper (TM)), and every 8 days when combined with Landsat 7 Enhanced Thematic Mapper Plus (ETM+). While the accuracy of ET estimates improves with coverage of two Landsat satellites, the temporal resolution provided by a single Landsat is sufficient in relatively cloud free areas, such as Nevada, to track crop phenology, agricultural management practices (e.g. cuttings and harvests), and ultimately crop ET [Tasumi et al., 2005; Cammalleri et al., 2014]. The study period of 2001 through 2011 includes several years when both Landsat 5 and Landsat 7 were fully functional (1999-2003). In addition, several large agricultural areas are located in areas of Landsat path overlaps (e.g. Mason Valley), creating twice the temporal

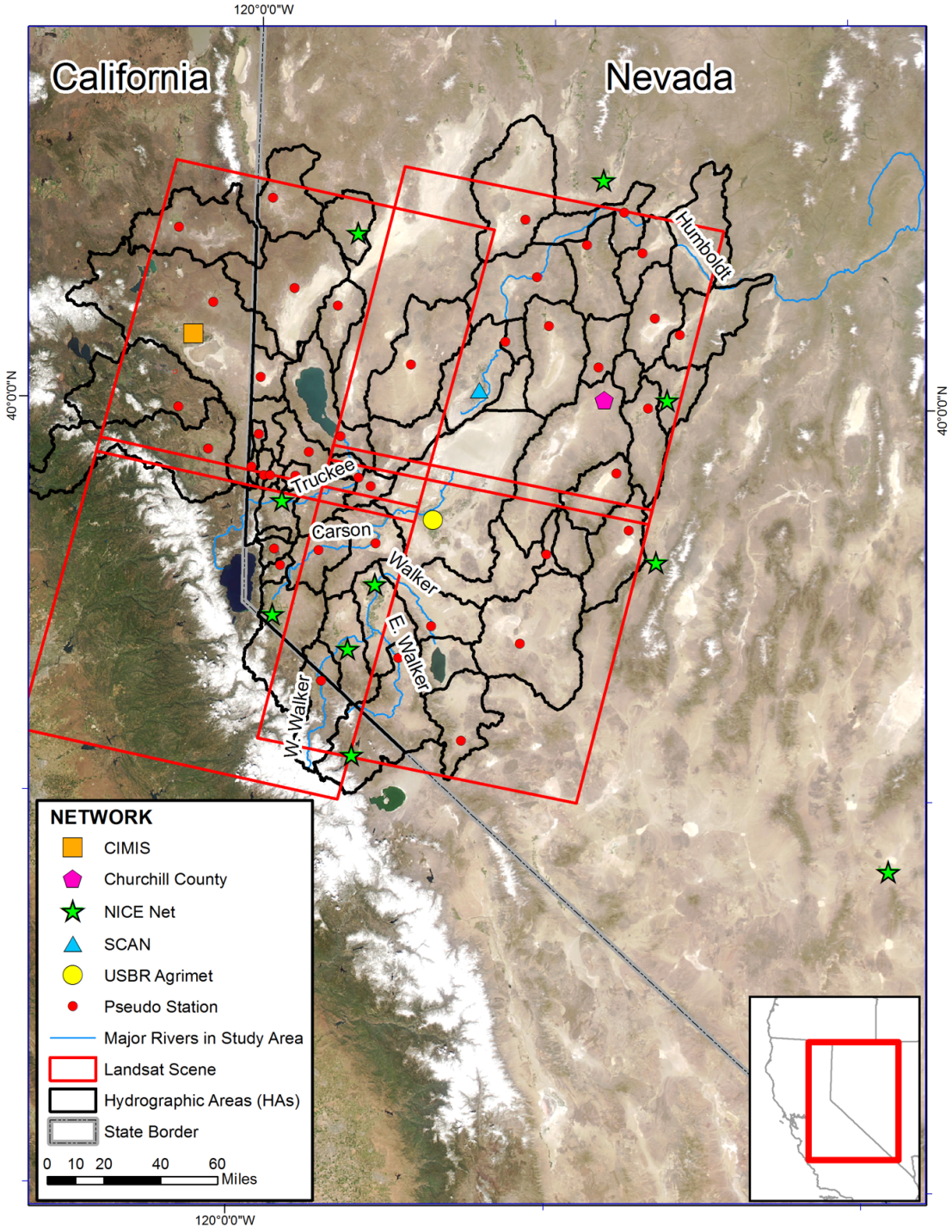


Figure 1. Study area contained within four Landsat scenes. Agricultural areas within Landsat scenes are summarized in this report. Agricultural weather stations and pseudo agricultural weather stations (where no actual stations exist but agricultural weather was estimated) are also illustrated.

coverage in those areas (Figure 1). Due to minimal cloud cover of northwestern Nevada, the probability of obtaining at least one cloud free image every 32 days is relatively high at 8 and 16 day return intervals, and ranges from 95 to 50 percent, respectively [Morton et al., 2016]. The high spatial resolution of Landsat allows for determination and evaluation of field scale crop ET and within-field variability useful for water and agricultural management [Tasumi et al., 2005; Tasumi and Allen, 2007; Anderson et al., 2012; Serbina and Miller, 2014].

Reference ET (i.e. evaporative demand of the atmosphere), surface temperature, albedo, vegetation indices, and land use / land cover are the primary input variables needed for the METRIC surface energy balance model. METRIC produces spatially explicit actual ET estimates that are generally accurate to within 10 to 20 percent [Allen et al., 2007a; Kalma et al., 2008]. The METRIC model has been successfully applied in Nevada by Morton et al. [2013] and Liebert et al. [2015], with results from these studies comparing well with micrometeorological station derived ET estimates. METRIC has also been recently applied by several state and federal agencies for estimating crop ET in New Mexico, Oregon, Wyoming, Montana, Nebraska, Colorado, and California [Hendrickx, 2010; Kjaersgaard and Allen, 2010; Anderson et al., 2012; Snyder et al., 2012; Serbina and Miller, 2014].

Weather stations located in agricultural areas, and bias-corrected and spatially disaggregated North American Land Data Assimilation System gridded weather data (METDATA) [Abatzoglou, 2013] (recently renamed to gridMET), provide weather variables of daily maximum and minimum air temperature ($T_{max}$ and $T_{min}$), actual vapor pressure ($e_a$), daily average solar radiation ($R_s$) and daily average wind speed at a 2 m height ($u_2$) needed for estimating reference ET. Reference ET is the estimated ET from a defined, standardized reference crop that is actively growing, not limited by soil moisture, and is at full cover and standardized height. Standardized reference crops in the U.S. are 0.5 m tall full-cover alfalfa, and 0.12 m tall clipped, cool-season grass as defined by the American Society of Civil Engineers (ASCE) Allen et al. [2005]. Reference ET ($ET_r$) is estimated in this study with the ASCE Standardized Penmen-Monteith (ASCE-PM) reference ET equation for an alfalfa reference crop [Allen et al., 2005]. Daily $ET_r$ is used in the METRIC process to calculate the instantaneous fraction of reference ET, and to perform time integration of actual ET between Landsat image acquisitions for estimating daily to annual ET totals. Seasonal and annual ET totals include ET from April through October and January through December, respectively. Spatially distributed precipitation data are derived from the Parameter Regression on Independent Slopes Model (PRISM; [Daly et al., 2002]) at 800 m spatial resolution, and used for estimating monthly and annual precipitation and net ET (ET minus precipitation) for agricultural areas within each HA.

Field scale monthly ET estimates are summarized by spatially averaging METRIC derived 30 m pixel resolution ET results to agricultural field boundaries based on the Common Land Unit (CLU) dataset [USDA Farm Service Agency, 2012]. CLU field boundaries were manually modified for each study year to accurately reflect changes in

agricultural land use and to eliminate or correct erroneous boundaries. Field scale monthly ET estimates serve as the primary dataset in which other datasets are populated and derived (e.g. geodatabase of ET, net ET, fraction of reference ET, and figures, tables, and appendices).

## METHODS

The following subsections describe weather data quality assurance and control (QAQC) and bias correction process, image preparation and cloud masking, field boundary delineation, and METRIC model application and post processing.

### WEATHER DATA PREPARATION AND QUALITY ASSURANCE AND CONTROL

Extensive preparation and QAQC of agricultural weather station data (Figure 1; Appendix 2) was performed prior to image processing and application of the METRIC model. Hourly and daily agricultural weather station data of air temperature, vapor pressure, relative humidity, solar radiation, and wind speed, were input into the software program, REF-ET [Allen, 2011] for QAQC and calculation of $ET_r$. REF-ET was used to visualize, filter, and make necessary corrections to weather variables according to the recommendations and guidelines of Allen [1996; 2008] and Allen et al. [2005]. For example, many weather variables are compared to theoretical limits or typical differences such as clear sky solar radiation (Figure 2) and 100 percent RH, and dew point depression ($T_{min} - T_{dew}$), respectively. Solar radiation corrections were the most common and are typically required due to possible debris on the pyranometer window, non-level base plate, sensor miscalibration or drift, or obstructions [Allen, 2008]. After extensive QAQC, $ET_r$ was calculated with filtered and corrected agricultural weather data for each weather station (Appendix 2).

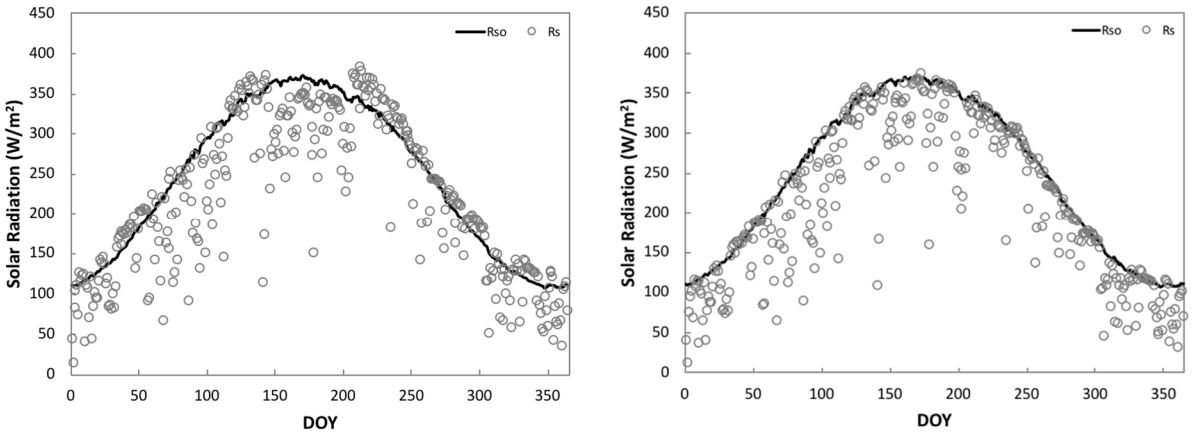


Figure 2. Example of 2005 Fallon AgriMet measured solar radiation ($R_s$) compared to theoretical clear sky solar radiation ($R_{so}$) before (left) and after (right) corrections.

Due to limited periods of record and lack of agricultural weather data for many HAs, simulated daily variables of $T_{max}$, $T_{min}$, $e_a$, $R_s$, and $u_2$ were acquired from 4 km spatial resolution METDATA [Abatzoglou, 2013] and used for computing $ET_r$ according to the ASCE-PM equation. Agricultural weather station derived $ET_r$ and coincident METDATA derived $ET_r$ time series were compared at monthly steps for common periods of record to assess potential biases. A positive bias in METDATA derived $ET_r$ was found at all 11 agricultural weather stations (Appendix 3) due to METDATA $T_{max}$, $T_{min}$, $T_{dew}$, and or $u_2$ being slightly warmer, dryer, and or higher wind speed than agricultural station measurements. A bias of this nature is typical when comparing ambient weather representative of the regional arid environment to observations collected within well-irrigated environments. For example, the Lovelock Soil Climate Analysis Network (SCAN) station is surrounded by well-irrigated pasture grass and alfalfa, and the monthly $ET_r$ at this station is consistently less than METDATA derived $ET_r$ (Figure 3). The primary input data source for the METDATA model, the North American Land Data Assimilation System [Rodell et al., 2015; Mitchell et al., 2004], does not account for irrigated areas and associated ET within land surface – boundary layer coupling processes [Ozdogan and Rodell, 2010]. Even in highly advective arid environments like northern Nevada, field scale land surface-atmospheric feedbacks have been well documented in irrigated areas surrounded by water-limited rangelands [Allen et al., 1983; Temesgen et al., 1999; Szilagyi and Schepers, 2014; Huntington et al., 2015]. Despite this common knowledge, practitioners and researchers alike routinely and erroneously apply

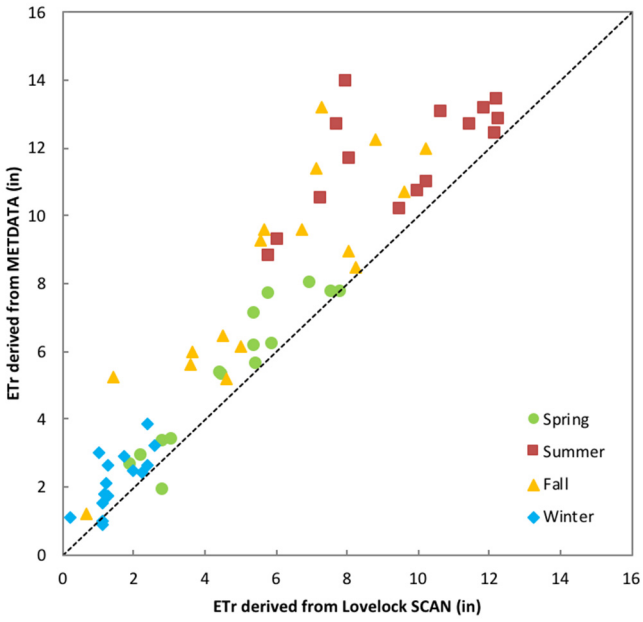


Figure 3. Lovelock USDA SCAN station derived monthly $ET_r$ and coincident METDATA derived monthly $ET_r$. The USDA SCAN station is surrounded by well-irrigated alfalfa and pasture grass.

$ET_r$ equations to estimate well-irrigated crop ET using arid or non-conditioned weather data. In order to bias correct METDATA, mean monthly ratios of station measured $ET_r$ to coincident METDATA $ET_r$ were computed at each agricultural weather station, and spatially distributed using inverse distance weighting. Spatial distributions of mean monthly bias correction factors were spatially averaged and assigned to study area HAs where no agricultural station based factors were available (Figure 4; Appendix 3). Mean monthly bias correction factors assigned to each HA (station based or interpolated) were applied to daily METDATA derived $ET_r$ for respective months.

Daily precipitation and $ET_r$ data from the Fallon AgriMet weather station were used in a soil-water balance model [Allen et al., 2011] to estimate rates of bare soil evaporation associated with rainfall prior to each Landsat image. Bare soil evaporation for the day of image acquisition must be included in the METRIC model calibration procedure as later described. The soil-water balance model was parameterized based on soil type, available water capacity, soil water content at field capacity, and plant wilting point. Soil data used for defining these parameters were obtained from the NRCS SSURGO soils GIS database, and spatially averaged to CLU-based field boundaries [NRCS, 2015; USDA Farm Service Agency, 2012].

### IMAGE PREPARATION AND LAND COVER

To ensure that Landsat pixels were without smoke, haze, clouds, shadows, cold air pooling, or image banding, it was necessary to visually inspect all available images within the study period. In total, 323 individual images were acquired and visually inspected, and most images within the same path were merged (i.e. acquired on the same day). If images were excessively contaminated, the images were excluded. In the case that limited clouds or other contamination features were present, masks were manually digitized to omit these areas from the image (Figure 5). In order to identify contaminated areas within each Landsat image, false color images based on visible, infrared, and thermal infrared bands were used to enhance the appearance of clouds, shadows, and haze.

Land cover information was used for parameterization of land surface roughness, emissivity, and energy balance functions within the METRIC model. Agricultural field boundaries were used to spatially average and summarize spatially distributed ET results for each field and HA. Land cover information was derived from a combination of datasets. CLU field boundaries representative of 2008 acreage [USDA Farm Service Agency, 2012], were manually modified for each study year based on visualizations of high resolution National Agricultural Imagery Program (NAIP) data. During years when NAIP was not available, Landsat false color composites for the year of interest were used in combination with NAIP and National Land Cover Database (NLCD) data from adjacent years. The end result was a complete annual field boundary dataset for each year of the study period. Field boundary changes most often occurred when traditionally flood or sprinkler line irrigated fields were converted to center-pivot irrigation systems, or new fields were put into production (Figure 6).

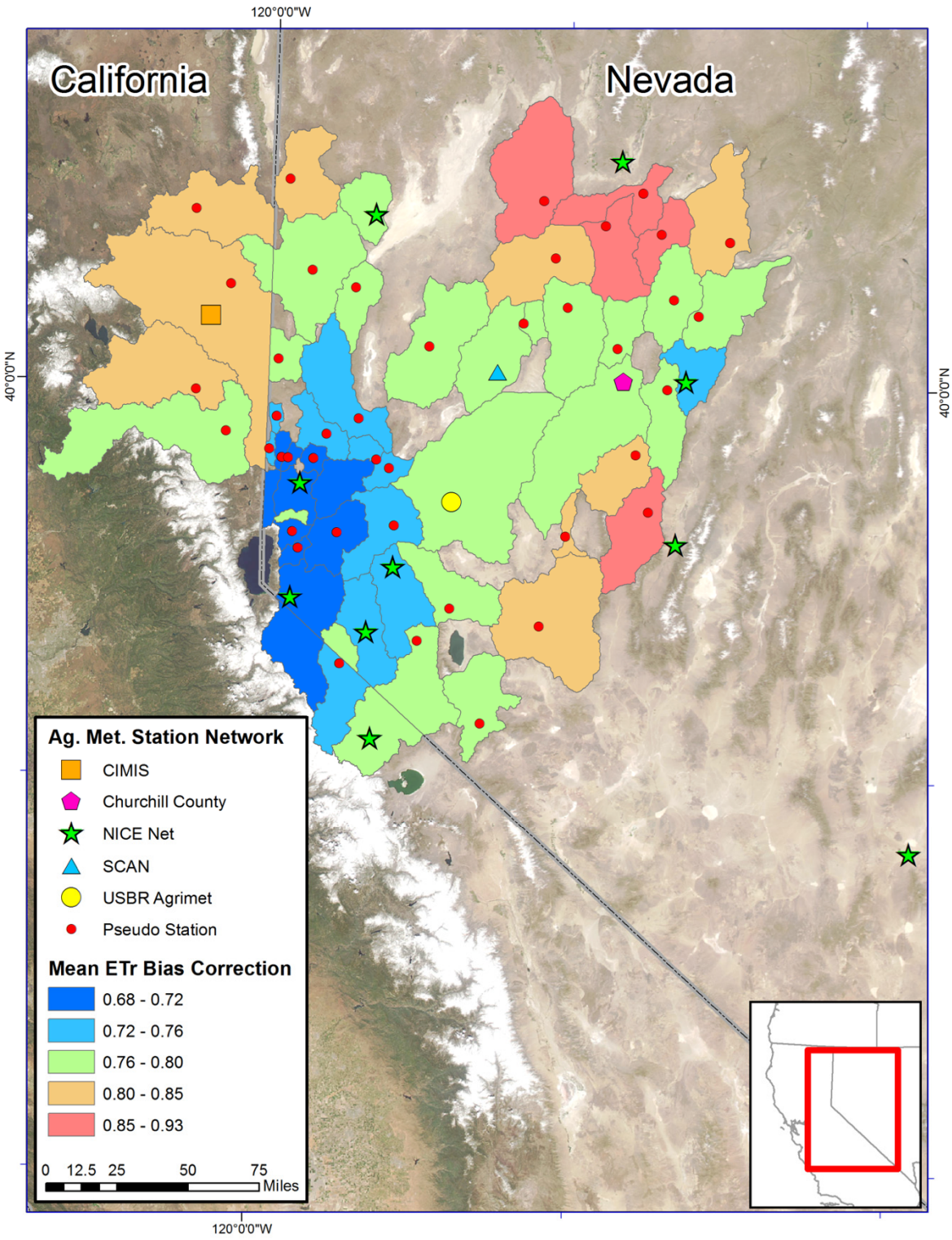


Figure 4. Spatial distribution of mean annual bias correction ratios of agricultural weather station derived $ET_r$ to METDATA derived $ET_r$. Mean monthly bias correction ratios were computed at stations, spatially interpolated between stations at 4 km spatial resolution using Inverse Distance Weighting, and then spatially averaged to HAs where no station based ratios were available.

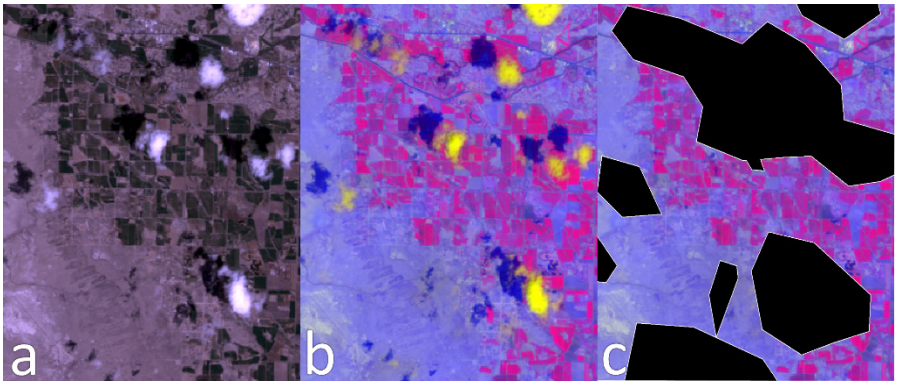


Figure 5. Example of cloud identification and masking. Potential contamination (due to smoke, haze, clouds, shadows, cold air pooling, or image banding) was identified by visualizing true color (a) and false color (with thermal and optical bands) (b) combinations. Cloud masks were manually digitized based on visually identified contamination areas (c). Any pixels within masked areas were not include in ET calculations.

Surface roughness used in the METRIC model was estimated from land cover data derived from three versions of NLCD [Homer et al., 2007, 2015; Fry et al., 2011], representing years 2001, 2006, and 2011. Detailed QAQC revealed that NLCD was not sufficiently accurate for the period of study due to misclassification and the omission of changes in land cover. To enhance NLCD agricultural land cover classes annual CLU-based field boundaries were integrated with NLCD resulting in a hybrid raster dataset. This hybrid land cover class dataset was used for estimating ground heat flux, surface roughness, and emissivity according to Allen et al. [2014].

## METRIC Model

Crop ET from 2001 to 2011 was estimated using the METRIC land surface energy balance model. METRIC computes instantaneous ET for each 30 m by 30 m Landsat pixel by estimating surface energy balance components and estimating latent heat flux as a residual of the energy balance as:

$$LE = R_n - G - H \quad (1)$$

where LE is the flux of latent energy (W/m$^2$), $R_n$ is the net radiation at the surface (W/m$^2$), G is the ground heat flux (W/m$^2$), and H is the sensible heat flux (W/m$^2$). METRIC estimates of $R_n$, G, and H were derived from Landsat at-surface reflectance and thermal radiance, vegetation indices, and measured incoming solar radiation and wind speed at the Fallon AgriMet weather station. Radiometric and atmospheric corrections to estimate at-surface reflectance, surface temperature, and albedo were made following Tasumi et al. [2008]. $R_n$ was estimated using Landsat derived albedo, emissivity, and estimates of shortwave and

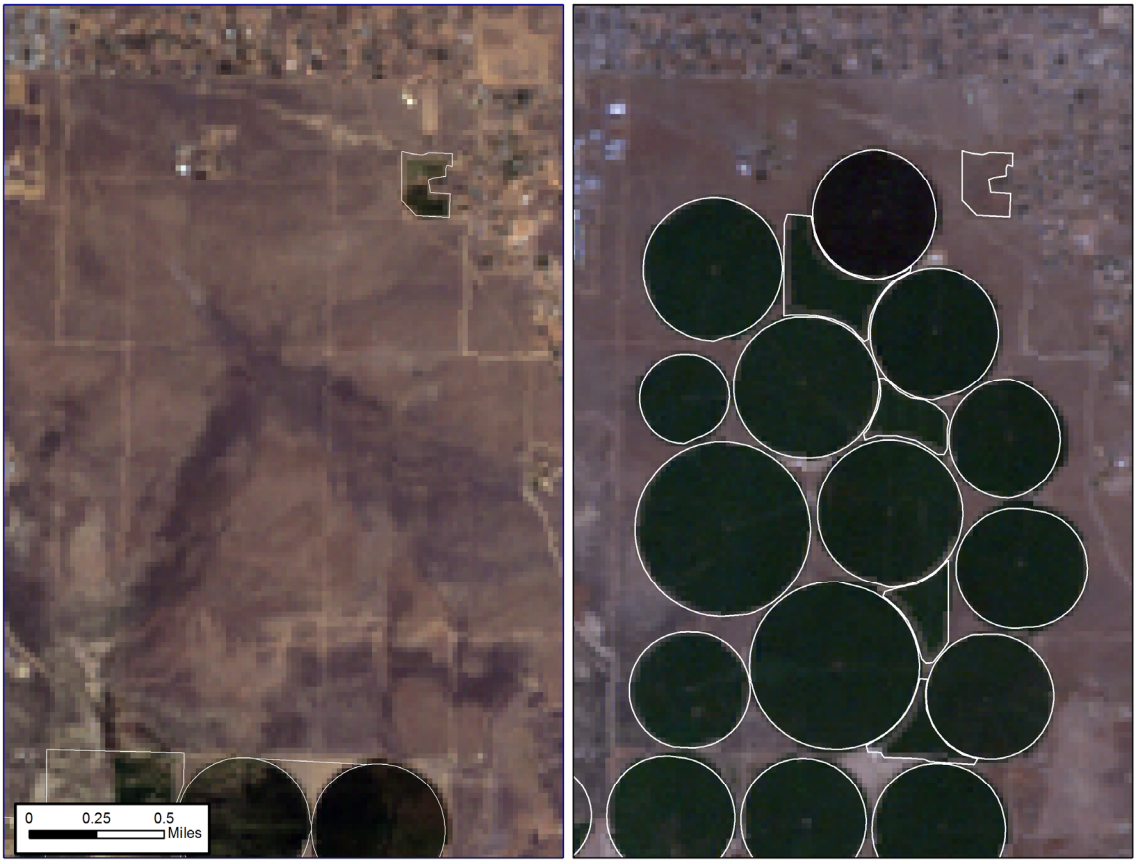


Figure 6. Agricultural field boundaries for Carson Valley for 2002 and 2011. Yearly field boundaries were developed due to agricultural land use changes that occurred during the study period.

longwave radiation. G was estimated as a function of land cover type, $R_n$, vegetation indices, and surface temperature. H was estimated as a function of surface temperature and atmospheric stability using an iterative Calibration using Inverse Modeling at Extreme Conditions (CIMEC) procedure [Allen et al., 2007a]. The CIMEC process factors out many of the biases in the energy balance, especially in surface temperature, estimated $R_n$, and inaccuracies associated with various model assumptions [Allen et al., 2007a].

The CIMEC procedure requires two calibration pixels, where ET can be easily approximated, so that the energy balance can be solved for H at locations that represent extreme ET conditions in the image. Once H is known at these extreme ET conditions, a linear relationship between Landsat surface temperature and the estimated temperature gradient (i.e. near surface air temperature difference (dT) just above the land surface) can be established and applied to the surface temperature image to estimate H, and therefore ET once $R_n$ and G are estimated for every pixel in the image. Calibration pixels for each image were manually selected based on a combination of image data such as surface temperature, the Normalized Difference Vegetation Index (NDVI), and albedo, to ensure selection of

representative extreme ET conditions (i.e. extreme low and high ET rates). The following three paragraphs detail the selection of calibration pixels.

The "hot pixel" calibration point is representative of the condition where there is substantial surface heating due to minimal ET (i.e. lack of evaporative and transpirative cooling). This calibration point ideally represents a location composed of bare, dry agricultural soil, and where surface temperature, albedo, and vegetation indices are generally homogenous within respective field boundaries. The criteria used to select hot pixels was based on recommendations outlined in the METRIC documentation [Allen et al., 2007a, 2014]. Hot pixels selected most often exhibit NDVI and albedo within the range of 0.11 to 0.2, and 0.17 to 0.23, respectively.

The "cold pixel" calibration point is representative of the condition of maximal evaporative cooling and ET, where all available energy ($R_n$-G) is consumed through LE, and H is zero or slightly negative. The condition commonly occurs when alfalfa is well-irrigated and is near or at full vegetation cover. Full cover alfalfa typically exhibits an albedo in the range of 0.18 to 0.24 and NDVI range of 0.76 to 0.84 during the growing season [Allen et al., 2014]. Images acquired early and late in the calendar year do not contain agricultural vegetation that is at full cover conditions, therefore, cold pixels selected during this timeframe were based on more relaxed albedo and NDVI criteria. Inaccuracies during this time have minimal impact on estimated annual ET due to low $ET_r$ during the non-growing season. Cold pixels were selected near centers of agricultural fields to prevent edge effects, and within fields that that were surrounded by similar land cover.

Once hot and cold calibration pixels were selected, respective ET rates were specified at each location. The ET rate representative of the cold pixel was assumed to be approximately zero to five percent greater than the $ET_r$ since the $ET_r$ does not account for ET from wet canopy or soil, due to recent irrigation [Tasumi et al., 2005; Allen et al., 2007a]. The ET rate representative of the hot pixel was assumed to be zero to 10 percent of the $ET_r$ to account for residual water content and evaporation common in agricultural soils. Estimates of bare soil evaporation using the model of Allen et al. [2011] were used to approximate the hot pixel evaporation rates associated with rainfall events prior to Landsat image acquisitions. If bare soil evaporation was estimated to be above 10 percent of $ET_r$, then the hot pixel ET rate was specified according to the estimated bare soil evaporation fraction of $ET_r$.

After all required input data was specified and organized for each Landsat image, the METRIC model was executed to compute instantaneous $R_n$, G, H, and LE. The instantaneous rate of ET at the time of image acquisition, $ET_{inst}$ (mm/hr) was calculated as

$$ET_{inst} = 3600 \times LE_{inst}/\lambda \quad (2)$$

where $LE_{inst}$ is the instantaneous latent heat flux derived from METRIC (W/m$^2$), $\lambda$ is the latent heat of vaporization for water (J/kg - i.e. the amount of energy absorbed when a

kilogram of water evaporates), and 3600 is a factor for time conversion from seconds to hours. While the $ET_{inst}$ is useful for many ecological and agricultural applications, such as detecting vegetation stress and water limitations, time integration of $ET_{inst}$ to estimate monthly and seasonal water use is needed for water resource applications. Time integration requires that a temporal index of $ET_{inst}$ be used to account for temporal variations in ET, caused primarily by changes in vegetation phenology, weather, and climate. This temporal index is developed by relating $ET_{inst}$ to the $ET_r$ at the time of image acquisition ($ET_{r\_inst}$). Hourly $ET_r$ computed at the Fallon AgriMet weather station was time interpolated to the exact image acquisition time (usually between 10:30am to 11:00am PST) to estimate $ET_{r\_inst}$. The ratio of $ET_{inst}$ to $ET_{r\_inst}$ is termed the instantaneous fraction of reference ET ($ET_rF$), otherwise known as the "crop coefficient". This ratio, which can be computed over many different time scales, is commonly used in agricultural engineering and hydrology to relate actual ET to reference ET in time and space [Allen et al., 1998; Allen et al., 2007a]. Temporal and spatial variability in $ET_rF$ is primarily the result of differences in water availability, crop type, phenology, vegetation roughness and turbulent effects, and vegetation cover and geometry (i.e. full cover vs. row crops). Simply put, the effects of weather and climate are incorporated into $ET_r$, whereas the effects that distinguish vegetated and bare surfaces from the reference surface are integrated into the $ET_rF$ [Allen et al., 1998; Hobbins and Huntington, 2016]. There are many biometeorological factors that determine ET, and the reference ET and $ET_rF$ approach integrates many of these factors [Allen et al., 2005; Bos et al., 2009].

Once $ET_rF$ was computed for every pixel in the image from Landsat derived $ET_{inst}$ and $ET_{r\_inst}$ derived from the Fallon AgriMet weather station, the ET rate for each 24-hour period ($ET_{24i}$) (mm/d) was estimated as

$$ET_{24i} = ET_rF_i \times ET_{r\_24i} \quad (3)$$

where $ET_{r\ 24i}$ is the 24-hour $ET_r$ total (mm/d) and $ET_rF_i$ is the fraction of $ET_r$ for day i (dimensionless). As previously described, because satellite imagery only provides instantaneous information at the time of acquisition, daily $ET_r$ is used to account for daily variations in atmospheric water demand. Two major assumptions in this approach are 1) the ratio of $ET_{inst}$ to $ET_{r\_inst}$ is fairly stable over a 24-hour period, where the $ET_rF$ ratio at the time of image acquisition is approximately equal to the 24-hour value, and 2) daily ET is proportional to daily $ET_r$. These assumptions are generally met for agricultural vegetation due to limited regulation of stomatal conductance, photosynthesis and transpiration [McNaughton and Jarvis, 1991; Allen et al., 1998; Tolk and Howell, 2001; Hunsaker et al., 2003; Cammalleri et al., 2014]. Non-cultivated vegetation in riparian and desert vegetation systems use stomatal regulation of transpiration as a physiological water use strategy, thus affecting the hourly and daily $ET_rF$, especially under water-limited conditions [Schulze et al., 1972; Collatz et al., 1991; Liebert et al., 2015]. Liebert et al. [2015] showed for a generally well-watered riparian system in southern Nevada, that although the hourly $ET_rF$ was highly

variable, the measured $ET_rF$ between 10:30 to 11:00 was similar to the 24-hour average, therefore using the instantaneous $ET_rF$ as a proxy for the 24-hour average resulted in satisfactory daily ET estimates. For regionally expansive and water limited native vegetation, the evaporative fraction (EF) approach is recommended over the $ET_rF$ approach to account for stomatal regulation, where EF equals the $LE_{inst}$ divided by the available energy ($R_n$-G) [Bastiaanssen et al., 1998]. For irrigated areas surrounded by arid environments, the use of the ASCE-PM equation to estimate $ET_r$ for time integration is recommended due to the ability of $ET_r$ to capture the potential effects of advection on ET (i.e. clothesline or oasis effect where H can be negative). Because this study focuses on agricultural areas surrounded by arid lands, the $ET_r$ * $ET_rF$ approach was applied for time integration of $ET_{24i}$ for each respective HA. This approach has been shown to be accurate over a wide range of irrigated agricultural conditions [Kalma et al., 2008; Gonzalez-Dugo et al., 2009; Anderson et al., 2012].

Time integration of $ET_{24i}$ to the monthly and seasonal time scale was performed as:

$$ET = \sum_{i=n}^{m} ET_r F_i \ * \ ET_{r\,24i} \quad (4)$$

where n and m are the first and last days of each month or season, respectively. In this study, n and m were specified to be the beginning and ending day of year (DOY) for each month to develop monthly ET totals each year. Temporal per-pixel linear interpolation of $ET_rF$ in-between satellite image dates was performed to estimate the daily value of $ET_rF$. Tasumi et al. [2005] and Liebert et al. [2015] show that this approach is effective for capturing changes due to growth stage, cuttings, harvests, and ultimately ET, however a minimum of one image per month is needed to capture these effects [Anderson et al., 2012, 2015]. As expected, errors in daily ET estimates due to per-pixel time interpolation of $ET_rF$ generally decrease as the interval between satellite overpass decreases. Due to northwestern Nevada experiencing many cloud free days during the growing season, it was rare to have less than one cloud-free image per month. For agricultural areas located in the overlap area between Landsat paths, cloud-free images with less than 8-day return times were frequent. The $ET_{r\,24}$ used to multiply by the daily interpolated $ET_rF$ was specific to each study area, and derived from METDATA bias corrected to locally measured agricultural weather station data so that local conditions were considered. Figure 7 illustrates an example where daily $ET_r$ is multiplied by time interpolated $ET_rF$ to estimate daily ET for an alfalfa field in Mason Valley, where alfalfa cuttings during the growing season were observed.

Winter months were affected by a decrease in the number of usable Landsat images due to increased cloud cover, atmospheric inversions, and/or snow cover. Huntington and Allen [2010] found that monthly non-growing season alfalfa and pasture grass soil water balance derived $ET_rF$ generally ranged from 0.1 to 0.3 in western Nevada, and is similar to the range estimated using non-growing season alfalfa ET rates derived from water balance lysimeter studies in Fallon [Guitjens and Goodrich, 1994]. In order to provide ET estimates

for periods outside the growing season, temporal interpolations were anchored with an assumed $ET_rF$ of 0.1 for the first day of the year and linearly interpolated to the $ET_rF$ derived from the first usable Landsat image of the calendar year. Conversely, the $ET_rF$ from the last usable Landsat image of the calendar year was linearly interpolated to the last day of the year, which was also assigned an $ET_rF$ of 0.1 (Figure 7a).

### APPLICATION AND POST-PROCESSING

Python programs outlined by Morton et al. [2013] were implemented to perform the METRIC process and time integration functions on multiple personal computers. Results were quality assured and controlled by evaluating statistics for each image through calculation and visualization of $ET_rF$ histograms, and calculation of the percentage of pixels above or below thresholds of 0.1 and 1.05, respectively. Large populations of pixels outside these extremes were cause for the re-calibration of METRIC through the re-selection of hot and cold pixels, and re-running METRIC until a reasonable distribution of $ET_rF$ was obtained. This iterative approach is similar to what is commonly employed during a automated calibration process of METRIC [Morton et al., 2013]. Once satisfactory results were obtained, per-pixel monthly, seasonal, and annual ET aggregations were made from 2001 and 2011. Per-pixel monthly, seasonal, and annual ET estimates were then spatially averaged to field boundary polygons to develop spatially averaged totals and area-weighted averages for all fields within each HA. A buffer distance of -30 m was applied to field polygons prior to spatially averaging ET rates to minimize pixel edge effects from impacting the spatial average. Spatially averaged ET rates derived from buffered polygons were assigned to original (i.e. non-buffered) field polygon areas and attribute tables for area-weighted average ET calculations and HA summaries. Area-weighted average ET rates for each HA were calculated as the total ET volume divided by the total field acreage for all fields within each HA. PRISM precipitation estimates were subtracted from field polygon spatially averaged ET rates to estimate monthly, seasonal, and annual net ET and area-weighted average net ET rates. The full amount of PRISM precipitation was subtracted from field polygon ET rates as a simple approximation of the lower bound of the net ET, and for QAQC and comparison to previously published NIWR rates assuming well-watered conditions. Some amount of precipitation is likely not consumed via ET due to runoff, deep percolation, and interception. Accurately estimating effective precipitation in each HA is complex and requires additional study. However, for further comparison purposes different approximations of effective precipitation and net ET (e.g. assuming 60 percent of annual precipitation in areas with significant sub-irrigation and runoff such as Carson Valley, Washoe Valley, etc.) could easily be made using the geodatabase of results.

## RESULTS

Estimates of ET, net ET, $ET_r$, and precipitation are summarized for the study period of 2001 through 2011 at monthly, seasonal (April – October), and annual time steps, and at

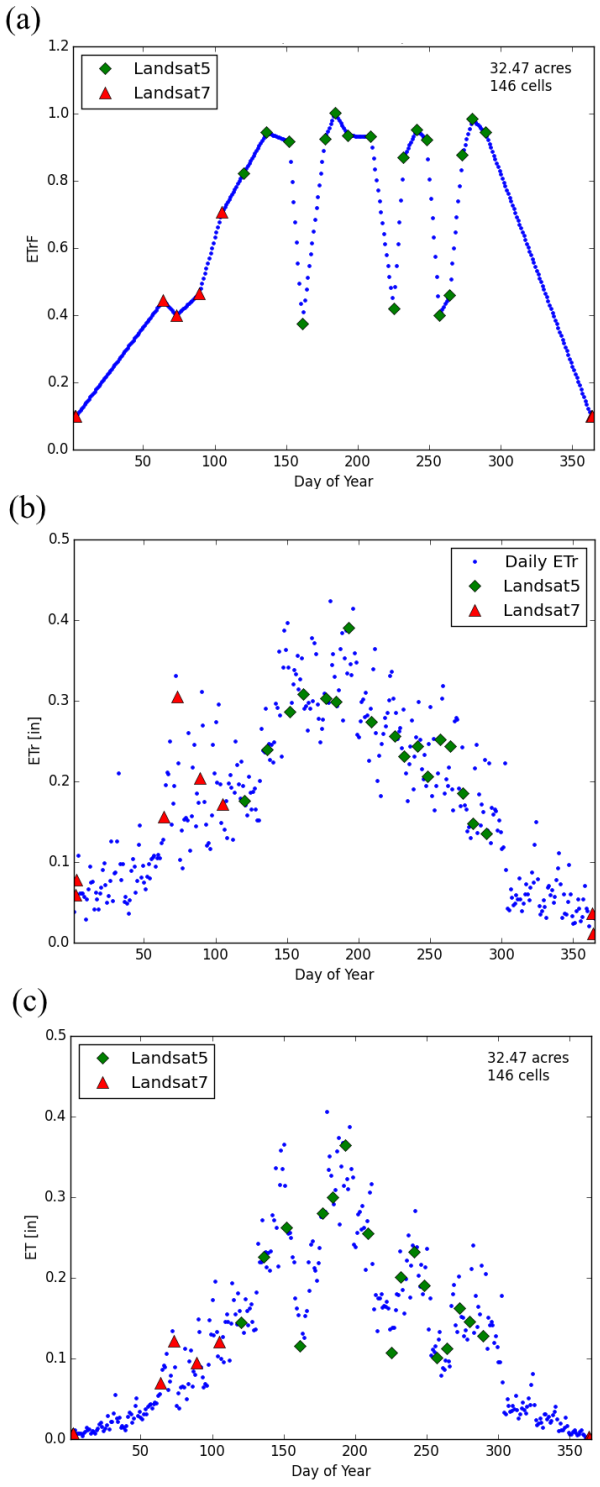


Figure 7. Time series of the fraction of reference ET ($ET_rF$), reference ET ($ET_r$), and crop ET for an alfalfa field in Mason Valley, where the daily time interpolated $ET_rF$ (a) is multiplied by the daily reference $ET_r$ (b) to estimate daily ET (c). The temporal distribution of $ET_rF$ illustrates crop development, cuttings, and dormancy.

field and/or basin scales depending on the variable. ET and net ET estimates are summarized by field and HA, and $ET_r$ and precipitation estimates are summarized by HA. Results are organized and illustrated multiple ways, including a ArcGIS geodatabase that contains all spatial and temporal data, map figures of field level seasonal and annual ET rates, histograms of annual ET vs. field acreage per HA, and matrix plots of monthly ET for each year. Area-weighted average annual ET rates for range from 1.25 to 3.98 ft/yr for all HAs, with the study period average of 2.89 ft/yr (Appendix 4a). Area-weighted average annual net ET rates range from -1.07 to 3.24 ft/yr for all HAs, with the study period average of 1.85 ft/yr (Appendix 4b). Figure 8 illustrates that there are large differences between METRIC derived ET (Figure 8a) and net ET (Figure 8b), and respective mean annual well-watered ET and NIWR rates reported by Huntington and Allen [2010] in many HAs. These differences represent the average difference between the potential crop ET of well-watered alfalfa and the actual crop ET derived from METRIC, which is a function of crop type, water availability, fallowing, crop-stress, disease, etc. Many of the study period maximum annual ET and net ET rates (shown as the top most whiskers) compare well to results from Huntington and Allen [2010], indicating that when ample water is available for irrigation, the actual ET derived from METRIC approaches well-watered ET and NIWR rates, as would be expected.

Yearly maps of field averaged annual and seasonal ET for all HAs are presented in Appendix 5 by HA and year. Figure 9 illustrates an example of field averaged seasonal ET for Lovelock for the years 2004 and 2008, which correspond to below and above average water years, respectively. Appendix 6 contains histograms of field averaged annual, seasonal, net annual, and net seasonal ET vs. field acreage for all HAs and study years. Figure 10 illustrates histograms of net annual ET vs. field area for Mason Valley and Lovelock Valley for years 2004 and 2008. The impact of below and above average water supply is clearly evident in Lovelock, however, Mason Valley maintains similar distributions of net annual ET due to supplemental groundwater pumping. Appendix 7 contains matrix plots of area-weighted average monthly ET distributions for each HA. Area-weighted average monthly ET distributions for Mason Valley and Lovelock are illustrated in Figure 11, and for Fish Springs Ranch and Fallon in Figure 12, which further illustrate how ET varies at monthly and annual timescales according to surface and groundwater availability and land use changes.

Annual and seasonal ET estimates summarized in this study compare well with previous estimates derived from micrometeorological, water balance lysimetry, and soil moisture depletion techniques. Figure 13 and Appendix 8 illustrate and list daily and seasonal average ET comparisons for respective time periods based on ET estimates from this study, and micrometeorological station derived ET estimates for alfalfa and pasture grass in Mason Valley and Carson Valley reported by Allander et al. [2009] and Maurer et al. [2006] and summarized by Morton et al. [2013]. METRIC ET estimates from this study are generally well within the error of micrometeorological station derived ET at daily and seasonal time scales (~10 to 20 percent; Appendix 8). Also, a historical well-watered average annual alfalfa

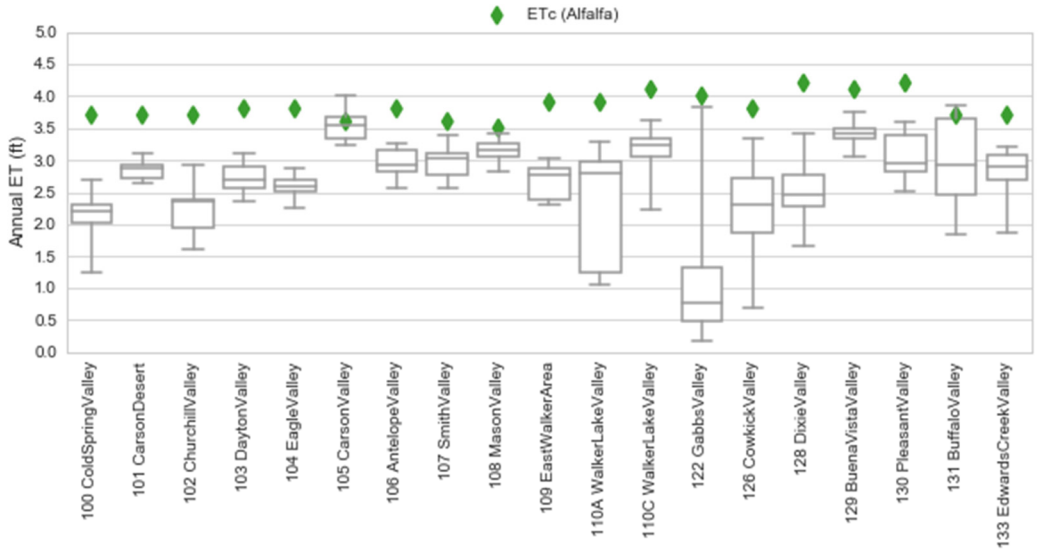


Figure 8a. Study period area-weighted average and interquartile, and maximum and minimum ET compared to annual average well-watered alfalfa ET estimates reported by Huntington and Allen [2010].

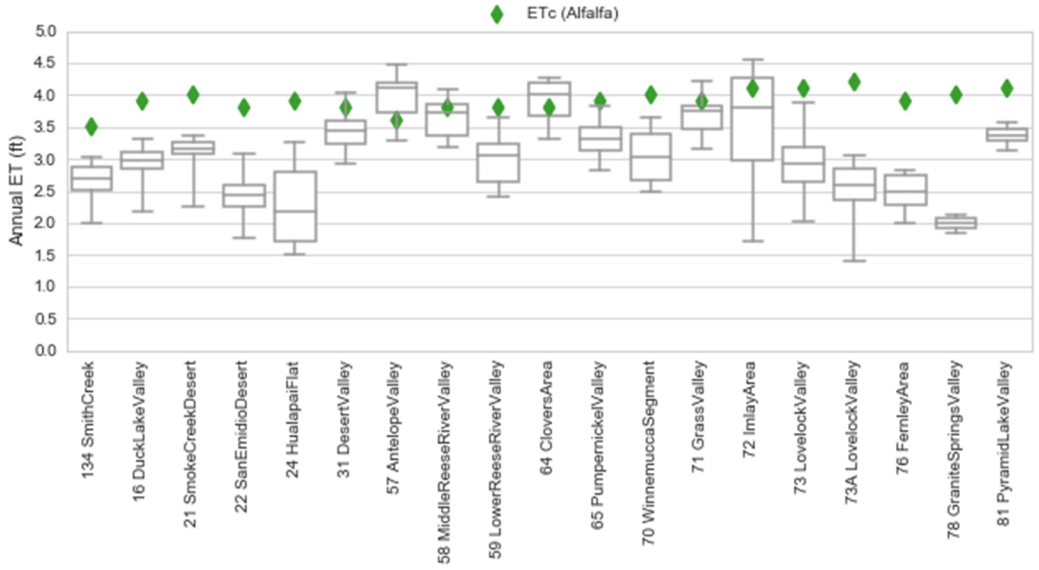


Figure 8a (cont.). Study period area-weighted average and interquartile, and maximum and minimum ET compared to annual average well-watered alfalfa ET estimates reported by Huntington and Allen [2010].

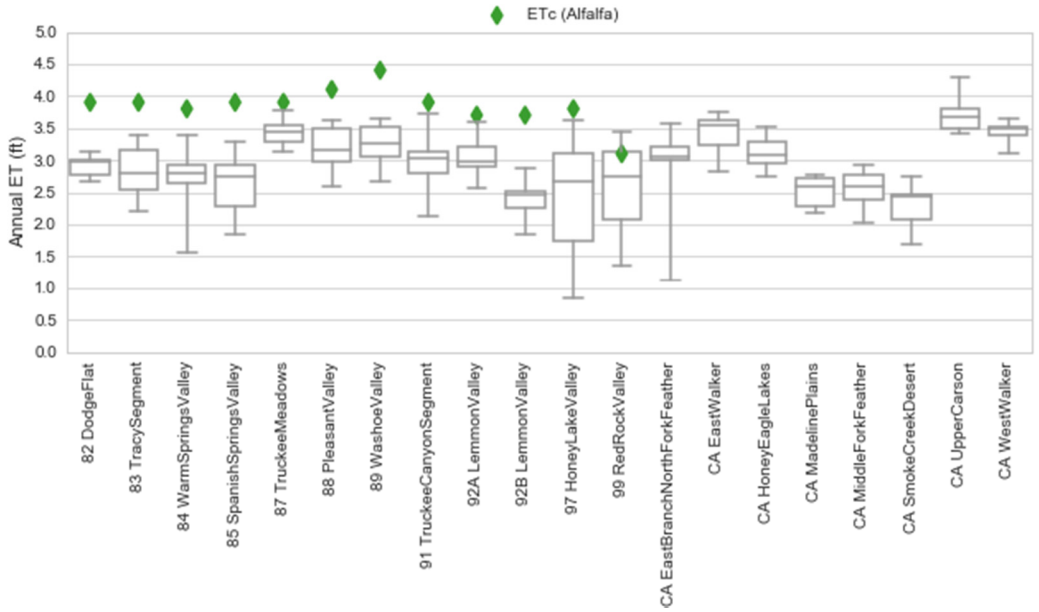


Figure 8a (cont.). Study period area-weighted average and interquartile, and maximum and minimum ET compared to annual average well-watered alfalfa ET estimates reported by Huntington and Allen [2010].

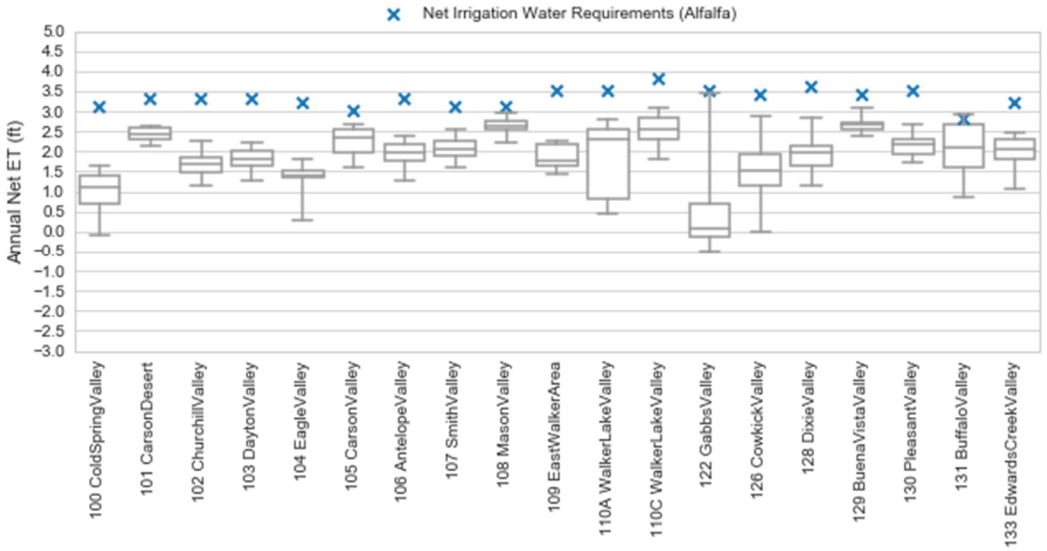


Figure 8b. Study period area-weighted average and interquartile, and maximum and minimum net ET (ET minus PPT) compared to annual average well-watered alfalfa Net Irrigation Water Requirement (NIWR) estimates reported by Huntington and Allen [2010].

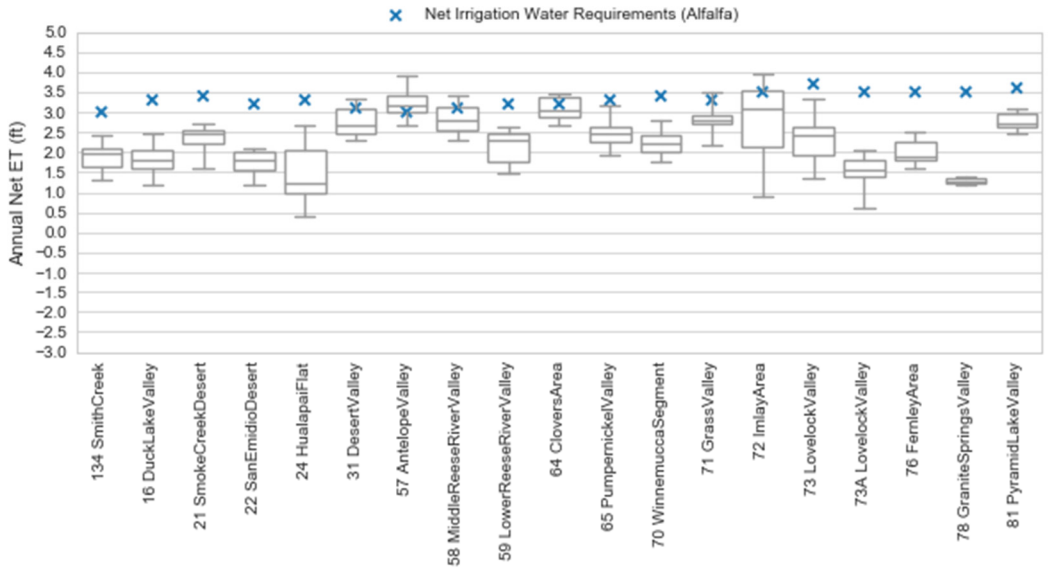


Figure 8b (cont.). Study period area-weighted average and interquartile, and maximum and minimum net ET (ET minus PPT) compared to annual average well-watered alfalfa Net Irrigation Water Requirement (NIWR) estimates reported by Huntington and Allen [2010].

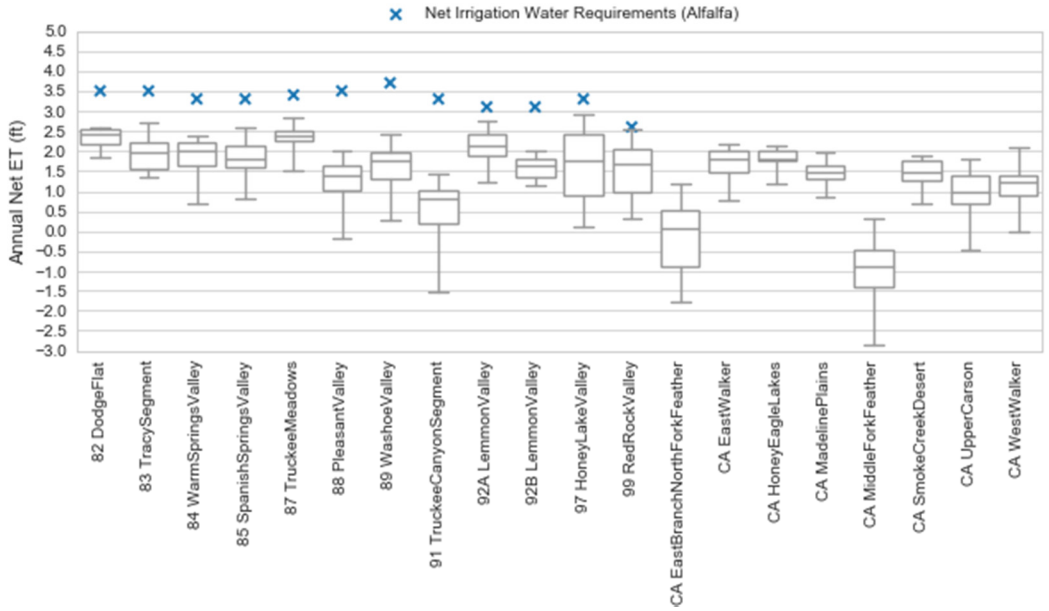


Figure 8b (cont.). Study period area-weighted average and interquartile, and maximum and minimum net ET (ET minus PPT) compared to annual average well-watered alfalfa Net Irrigation Water Requirement (NIWR) estimates reported by Huntington and Allen [2010].

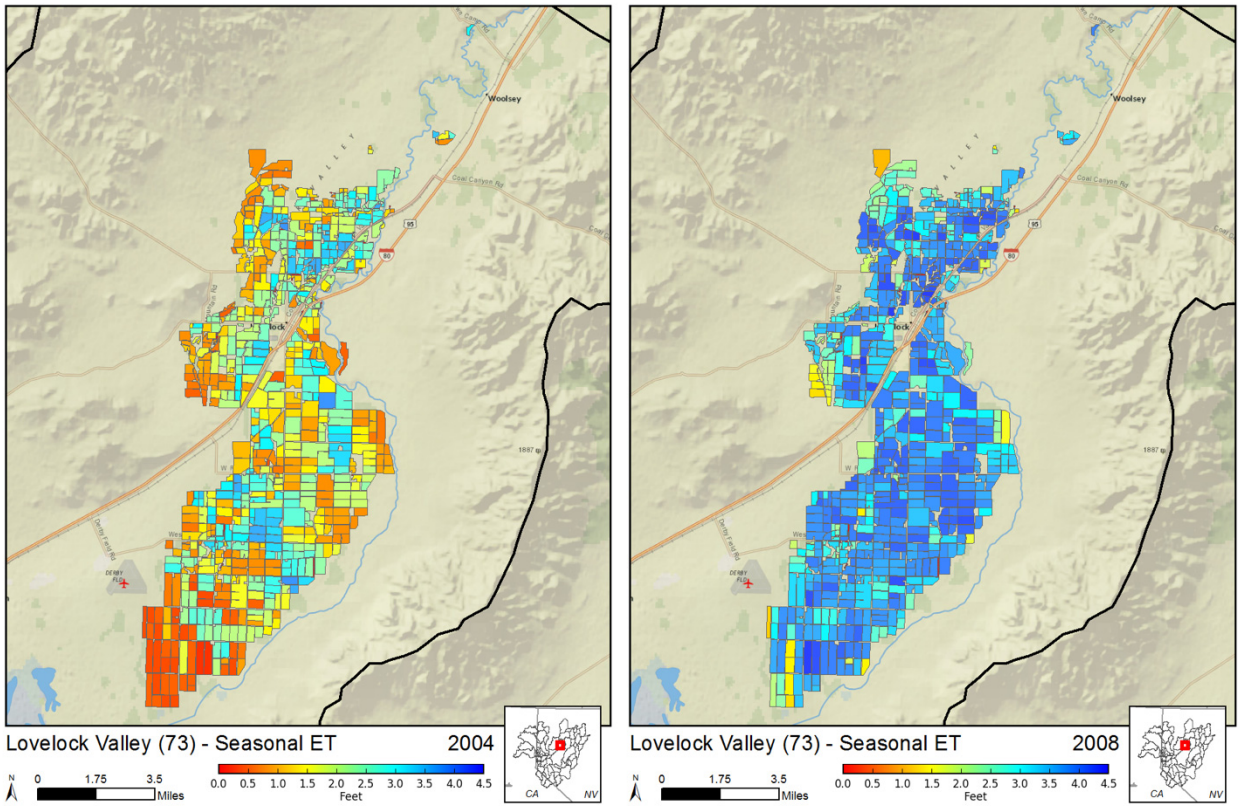


Figure 9. Spatial distribution of field averaged seasonal ET for Lovelock Valley for 2004 and 2008, which correspond to dry and wet years, respectively.

ET estimate of 3.70 ft/yr, derived from water balance lysimetry techniques in Fallon (Carson Desert) [Guitjens and Mahannah, 1977; Rashedi, 1983; Guitjens and Goodrich, 1994], compares well to the METRIC derived area weighted well-watered average ET rate in Fallon of 3.57 ft/yr.

METRIC derived annual ET and net ET rates representative of well-watered conditions were approximated as the top 25th percentile of field averaged ET rates, and compare well with previous $ET_r$ – crop coefficient and daily soil water balance model estimates of well-watered annual crop ET and NIWR estimates for most HAs [Huntington and Allen, 2010] (Figure 14a, b; Appendix 9). While a comparison of ET for respective years was not possible due to non-overlapping study periods, comparing well-watered mean annual alfalfa ET estimates to top 25th percentile of field averaged ET estimates from this study is useful for evaluating general similarities for respective HAs. For example, Huntington and Allen [2010] reported mean annual alfalfa ET to be 3.5, 3.7, and 4.1 ft/yr, for Mason Valley, Fallon, and Lovelock, respectively. These estimates are within 20 percent of the top 25th percentile average annual ET estimates from this study of 3.93, 3.57, and 3.79 ft/yr for Mason Valley, Fallon, and Lovelock, respectively. Differences between METRIC derived top

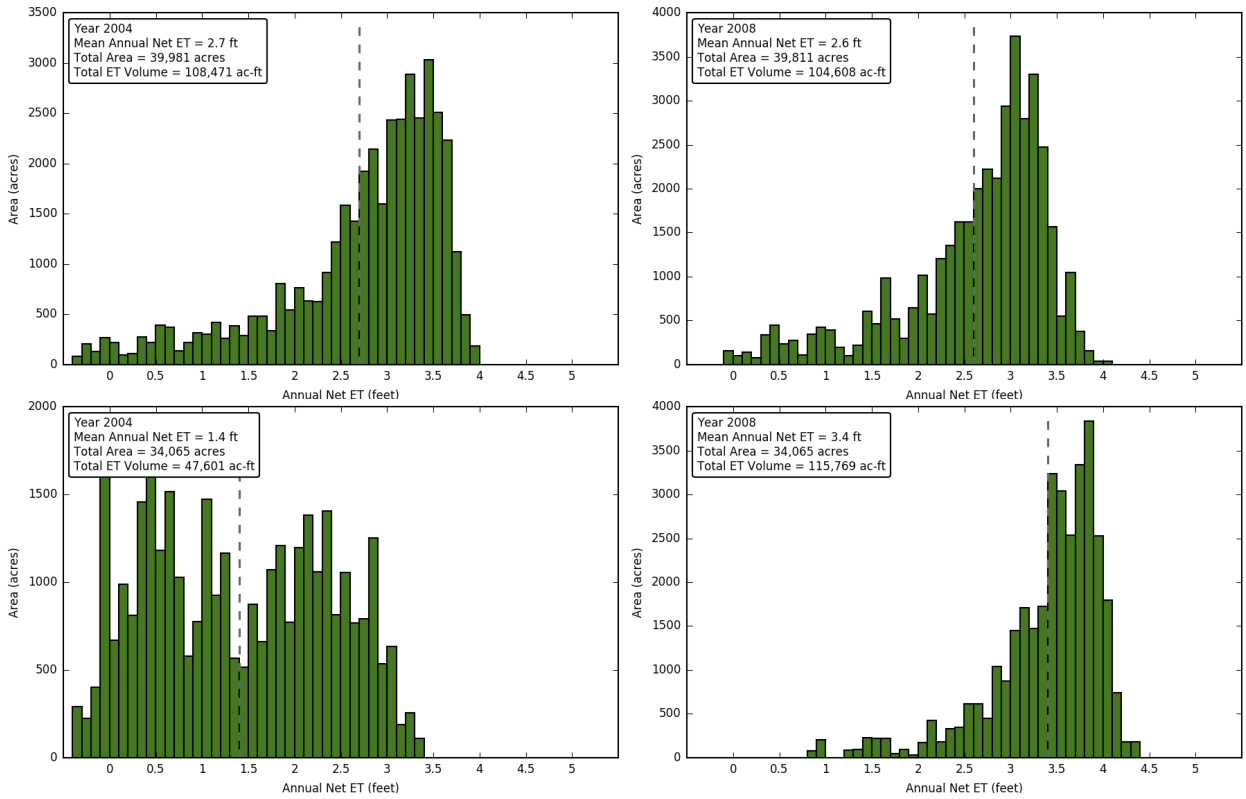


Figure 10. Histograms of net annual ET vs. field acreage for Mason Valley (top row) and Lovelock Valley (bottom row) for years 2004 and 2008. The impact of drought is clearly evident in Lovelock, however, Mason Valley maintains similar distributions of ET both years due to supplemental groundwater pumping.

25th percentile average annual ET and net ET reported in this study and respective mean annual alfalfa ET and NIWR estimates reported by Huntington and Allen [2010] are likely due to multiple factors, including differences in study period length and timing (e.g. 2001-2010 vs. ~1978-2007), inaccuracies and differences in reference ET and modeling approaches, areas included (e.g. inclusion of numerous sub-irrigated pasturelands / wetlands in the METRIC analysis such as in Mason Valley and Carson Valley) differences in crop type, phenology, growing season lengths, harvest times, and calculation of effective precipitation. Given that the majority of crop acreage grown within the study areas is alfalfa (i.e. a high water consuming crop), it is reassuring that that alfalfa ET estimates from Huntington and Allen [2010] generally compare well with top 25th percentile average annual ET rates reported in this study.

## DISCUSSION

To assess how agricultural ET varies across different study area HAs, METRIC derived ET estimates were evaluated with respect to drought and land use changes through

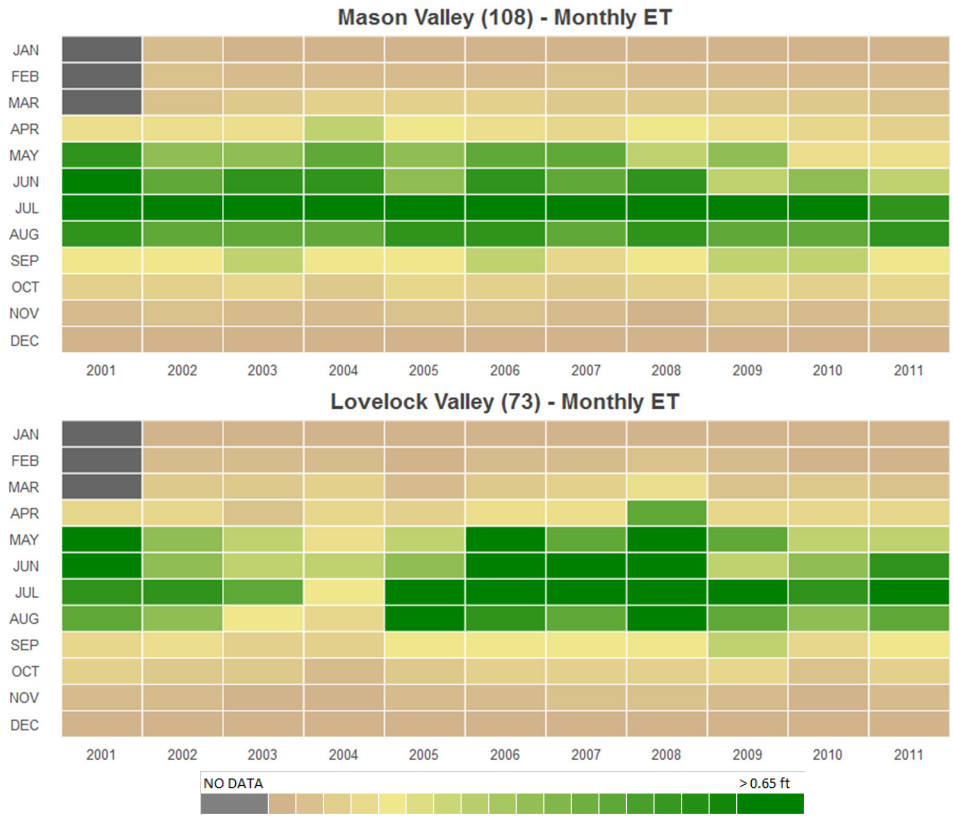


Figure 11. Matrix plots of field area-weighted average monthly ET over the study period for Mason Valley (top) and Lovelock Valley (bottom). Annual monthly distributions of ET illustrate monthly an annual variability according to surface and groundwater availability, where Lovelock ET is more variable due to drought and lack of supplemental groundwater pumping.

illustrations of spatio-temporal ET distributions. Lovelock, Fish Springs Ranch (i.e. Honey Lake Valley), Fallon, and Mason Valley HAs were selected to highlight how differences in surface and groundwater rights, land use changes, and upstream storage can impact ET in space and time. Impacts from drought are clearly demonstrated by evaluating and discussing the temporal distributions of METRIC derived monthly ET estimates for select HAs. Temporal ET distributions indicate that field area-weighted average monthly ET rates were much more variable from 2001- 2011 for Lovelock and Fish Springs Ranch than for Fallon and Mason Valley (Figures 11 and 12). Fallon and Mason Valley exhibited among the highest mean and lowest range in annual ET rates, while Lovelock and Fish Springs Ranch exhibited among the lowest mean and highest range in annual ET rates over the study period (Figure 8). Lovelock is almost entirely dependent on the Humboldt River for surface water irrigation due to poor groundwater quality within the basin. Rye Patch Reservoir provides limited upstream storage for irrigation water throughout the growing season, and due to the limited capacity of the reservoir (213,000 acre-feet of water storage [Hoffman et al., 1990],

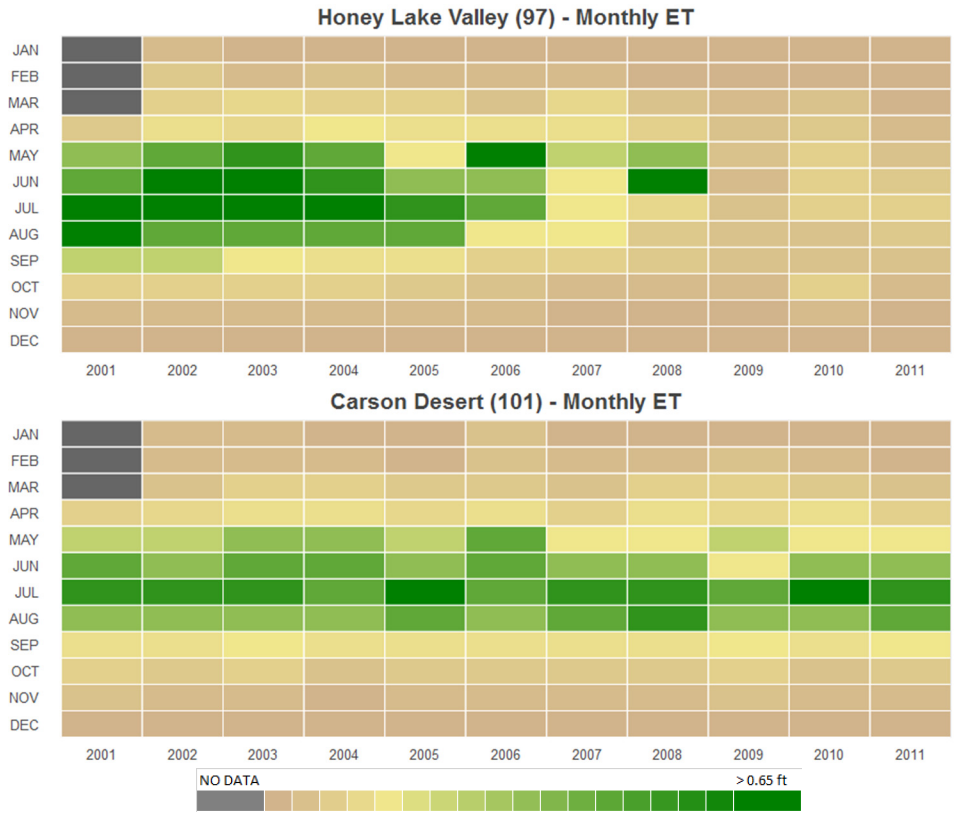


Figure 12. Matrix plots of field area-weighted average monthly ET over the study period for Fish Springs Ranch – Honey Lake Valley (top) and Fallon (bottom). Change in land use in 2009 (fallowing) at Fish Springs Ranch reduced ET, whereas Fallon ET has relatively low annual variability due to upstream reservoir storage and irrigation during drought years.

extended droughts often result in little to no delivery of irrigation water to Lovelock. The impact of drought is clearly evident in Lovelock during the early 2000s, and increasing with severity from 2001-2004 (Figure 11). Another period of drought occurred from 2009 through 2011, corresponding to a second period of reduced ET in Lovelock (Figure 11).

In 2000, Fish Springs Ranch located in Honey Lake Valley was acquired by Vidler Water Company to export up to 13,000 acre-feet of groundwater irrigation rights associated with the property [Vidler Water Company, 2015]. A change in the manner of use, from irrigation to municipal, and an inter-basin transfer from the Honey Lake HA to the Lemmon Valley HA was approved by the Nevada State Engineer in 2000. Figure 12 illustrates a sharp decline in ET in 2005, when irrigation largely ceased and much of the ranch was fallowed. Vidler continued to operate the ranch with minimal irrigation until 2007, when water works were installed to transfer pumped groundwater into Lemmon Valley via a pipeline. After 2007, ET rates fell to background levels due to the fallowing of all irrigated lands.

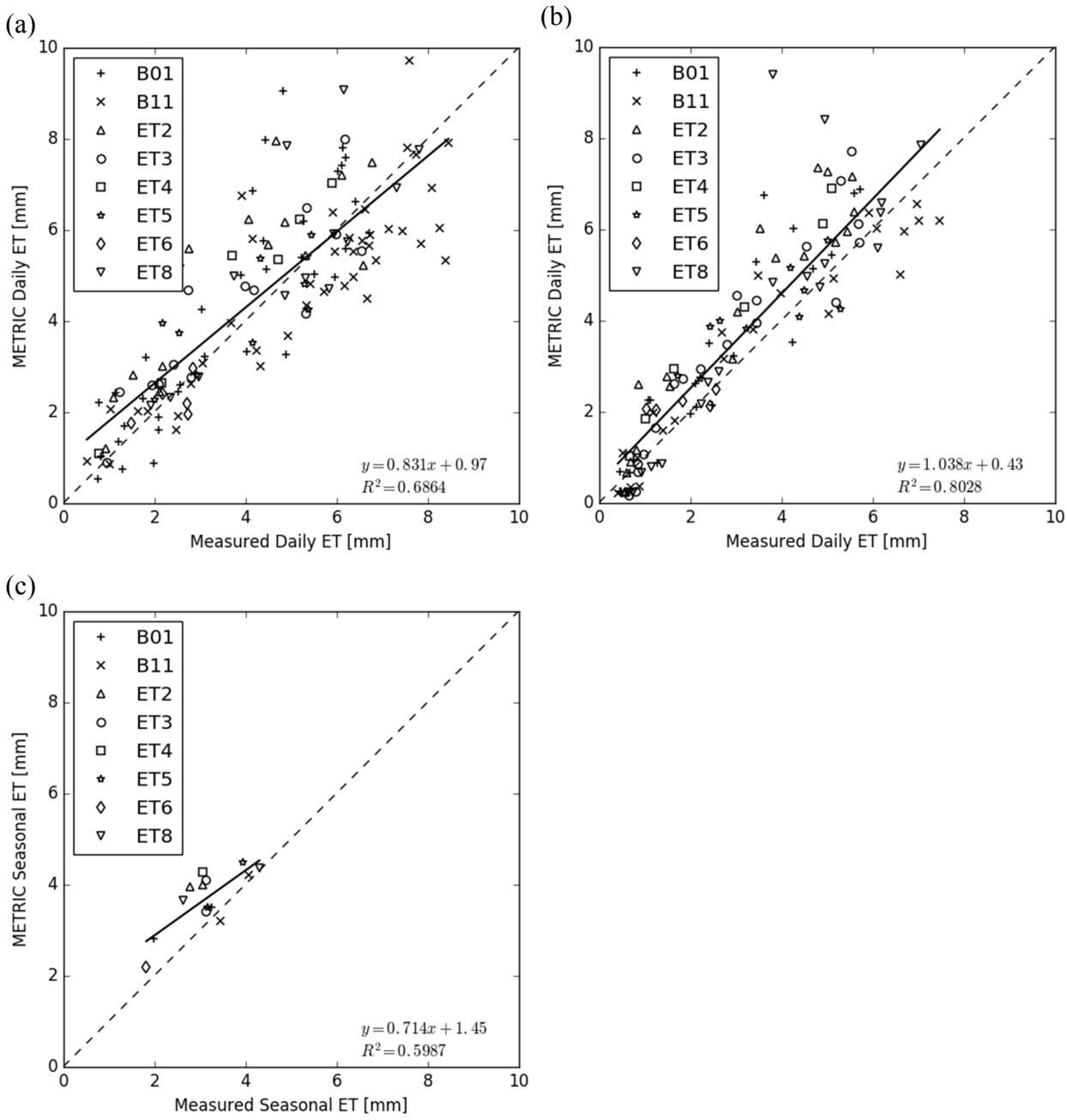


Figure 13. Comparisons of METRIC derived ET and micrometeorological station derived ET for alfalfa and pasture grass in Mason Valley and Carson Valley reported by Allander et al. [2009] and Maurer et al. [2006] and summarized by Morton et al. [2013]. Comparison plots are daily ET for Landsat image acquisition days (a), mean daily ET for each month (b), and mean daily ET for the seasonal measurement period (c).

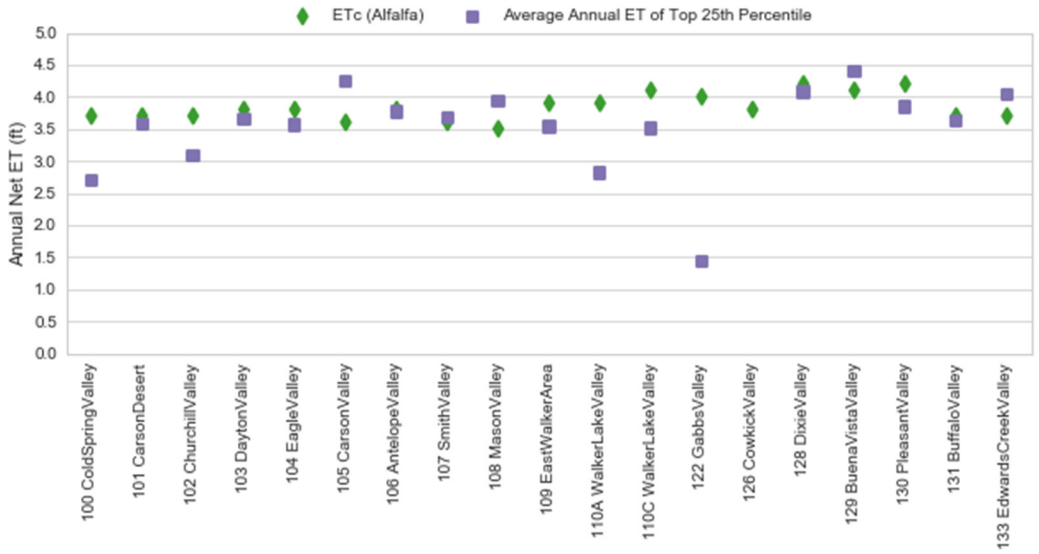


Figure 14a. Study period area-weighted average average top 25 percentile ET compared to annual average well-watered alfalfa ET estimates reported by Huntington and Allen [2010].

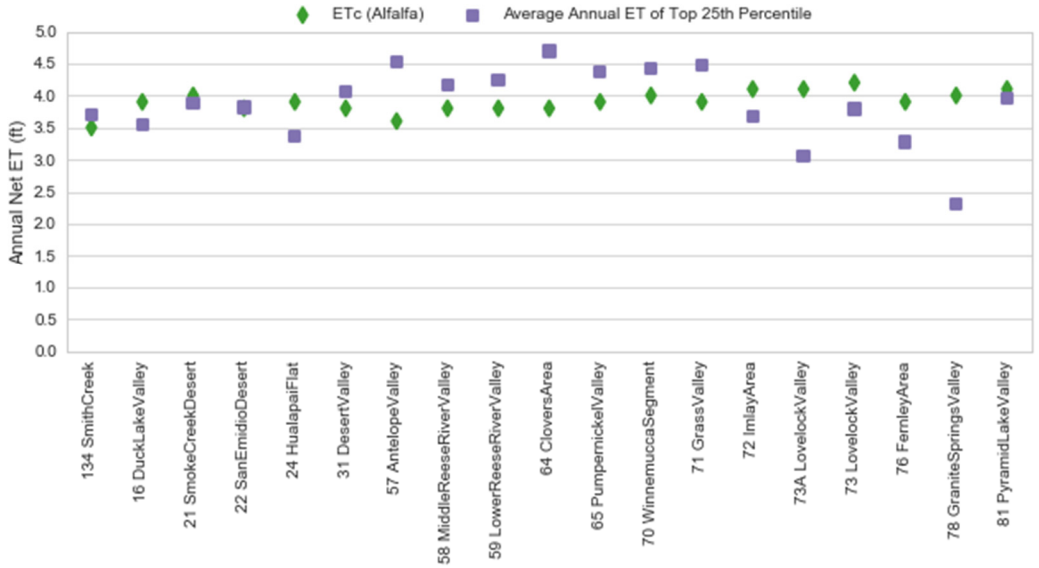


Figure 14a (cont.). Study period area-weighted average average top 25 percentile ET compared to annual average well-watered alfalfa ET estimates reported by Huntington and Allen [2010].

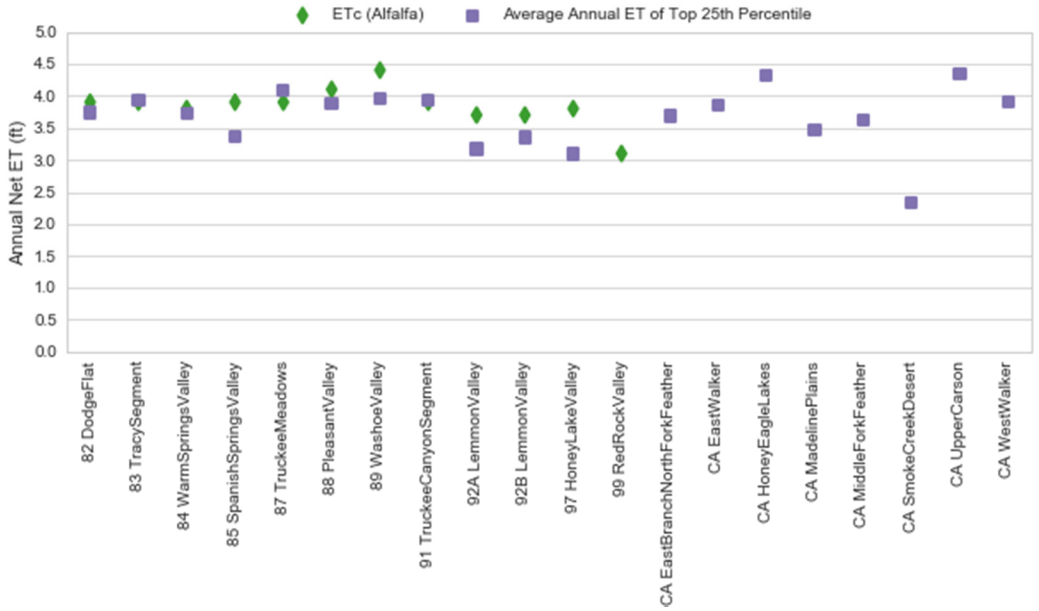


Figure 14a (cont.). Study period area-weighted average average top 25 percentile ET compared to annual average well-watered alfalfa ET estimates reported by Huntington and Allen [2010].

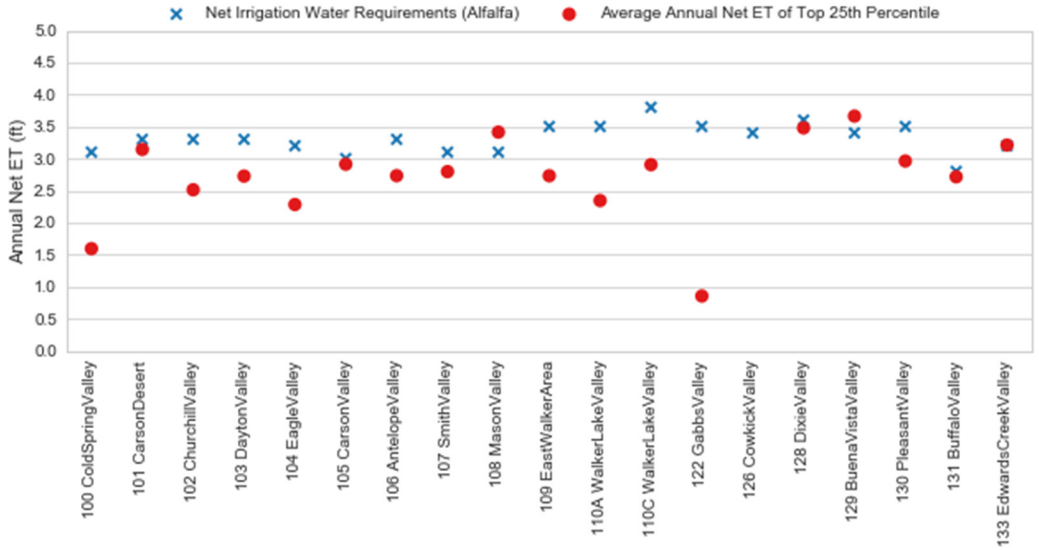


Figure 14b. Study period area-weighted average top 25 percentile net ET (ET minus PPT) compared to annual average well-watered alfalfa Net Irrigation Water Requirement (NIWR) estimates reported by Huntington and Allen [2010].

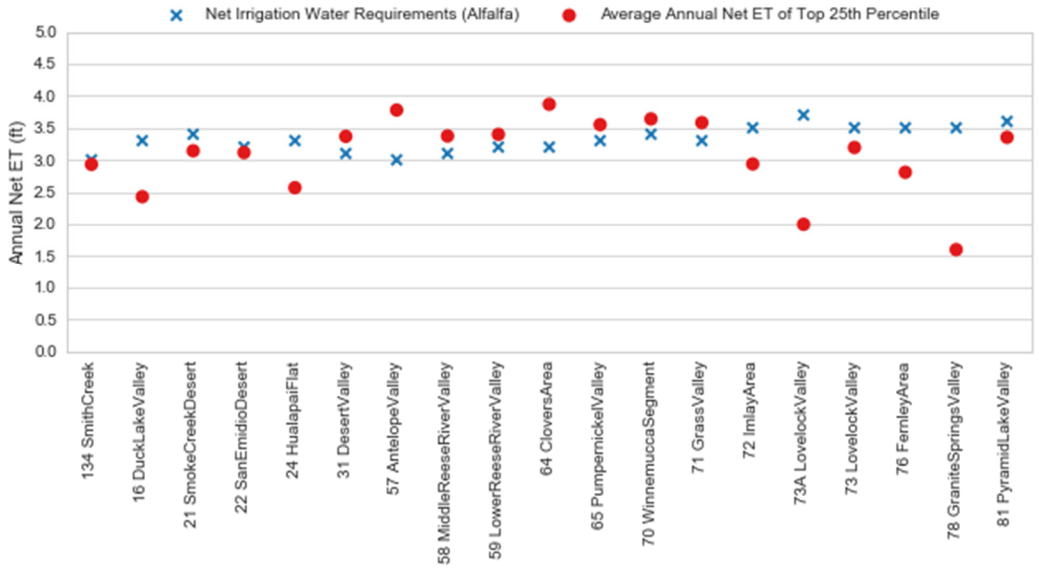


Figure 14b (cont.). Study period area-weighted average top 25 percentile net ET (ET minus PPT) compared to annual average well-watered alfalfa Net Irrigation Water Requirement (NIWR) estimates reported by Huntington and Allen [2010].

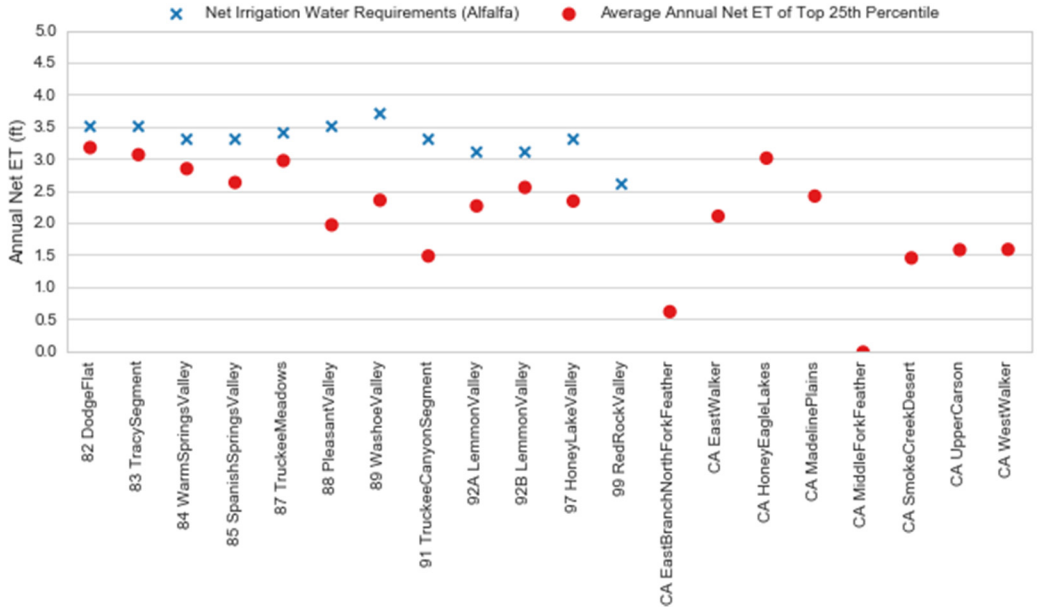


Figure 14b (cont.). Study period area-weighted average top 25 percentile net ET (ET minus PPT) compared to annual average well-watered alfalfa Net Irrigation Water Requirement (NIWR) estimates reported by Huntington and Allen [2010].

Both Mason Valley and Fallon ET rates have relatively low seasonal variability from 2001-2011 primarily due to supplemental groundwater pumping and upstream storage, respectively (Figure 11 and 12). Mason Valley receives water primarily from surface water diversions of the Walker River, and secondarily from supplemental groundwater pumping during periods of drought. Fallon lacks supplemental groundwater pumping, however, it is relatively well-buffered from drought due to ample upstream storage on the Truckee River and Carson River systems. In Mason Valley and Fallon, each year begins with minimal ET due to low $ET_r$, followed by an increase in ET during crop green-up and development stages of April and May, with ET reaching a maximum during June and July during full canopy cover and maximum $ET_r$. ET rates decline sharply in September due to alfalfa, and onion and garlic harvests in Mason Valley, and remain at minimal levels until April the following spring. This seasonal distribution of ET reflects the seasonal distribution of $ET_r$ combined with initial development, maturity, harvest, and dormancy crop stages for well-irrigated agriculture in Nevada. The seasonal ET distribution is relatively consistent from year to year, even during prolonged periods of drought that occurred from 2001-2003 and 2009-2010 (Figure 11).

The spatial distribution of seasonal ET during dry and wet years is primarily a function of surface and groundwater availability, and water rights priority. For example, differences in seasonal field scale ET from a dry (2004) to a wet (2008) year is large, and generally uniform for most fields in Lovelock due to limited surface water supply, absence of groundwater pumping, and irrigation district water rights (Figure 9). Fairly uniform reductions are common for irrigation districts where water right priorities are similar across the district. In Mason Valley, where water rights are commonly a mix of both surface water and groundwater, and with large ranges in priority dates, the magnitude and spatial uniformity of reduced ET is not as evident when comparing wet and dry years. For example, Figure 15 illustrates the spatial distribution of seasonal ET in Mason Valley for 2002 and 2006, which were dry and wet years, respectively. During 2002, high ET fields are presumably concentrated in areas where senior surface water rights exist, and where groundwater pumping is a primary or secondary water right and used during times of drought. ET changes during wet and dry years are more pronounced in Fallon due to the lack of supplemental groundwater, however, not as extreme as Lovelock due to ample upstream storage on the Truckee and Carson River systems. Figure 16 illustrates the spatial distribution of Fallon seasonal ET for 2009 and 2010, which were dry and wet years, respectively. The prolonged drought during the late 2000s caused a shortage of irrigation water by 2009. However, in 2010 reservoir storage deficits were replenished, and irrigation demands were generally met. Figure 16 illustrates higher ET for some fields, and higher spatial variability in 2009 than 2010. This is the result of higher $ET_r$ in 2009, and potentially fields with higher water right priorities that received full or nearly full water allocations. In 2010 ET was more spatially uniform than 2009, a likely result of ample water supply for the entire irrigation district.

While many water budget and groundwater modeling studies in Nevada assume that crop ET rates are temporally and spatially constant [Maurer and Berger, 2006; Allander et al., 2009; Lopes and Allander, 2009; Carroll et al., 2010; Halford and Plume, 2011; Yager et al., 2012], results from this study indicate that temporal and spatial distributions of crop ET are highly variable in space and time, and should therefore be considered when developing water budgets, surface and groundwater models, and impact assessments. For example, based on the work presented in this study Carson Valley crop ET volumes vary by approximately 29,000 ac-ft/yr from a wet year (2006) to a dry year (2009), which equates to over one and a half times the average groundwater pumping of 17,000 ac-ft/yr [Maurer and Berger, 2006]. Incorporating spatial and temporal ET variability into surface and groundwater budget and modeling studies will more realistically represent one of the largest water budget components of many HAs in northwestern Nevada, the crop ET. Landsat-based remote sensing is currently the only way to accurately assess historical crop ET at field scales and over large areas and long time periods. Moreover, evaluating crop ET over long time histories will improve our understanding of potential agricultural impacts due to climate, drought, water rights and transfers, and land use changes.

## LIMITATIONS

The methods applied to estimate ET in this report are not absent of uncertainties and limitations. Potential sources of uncertainty include METRIC inaccuracies, inaccuracies in

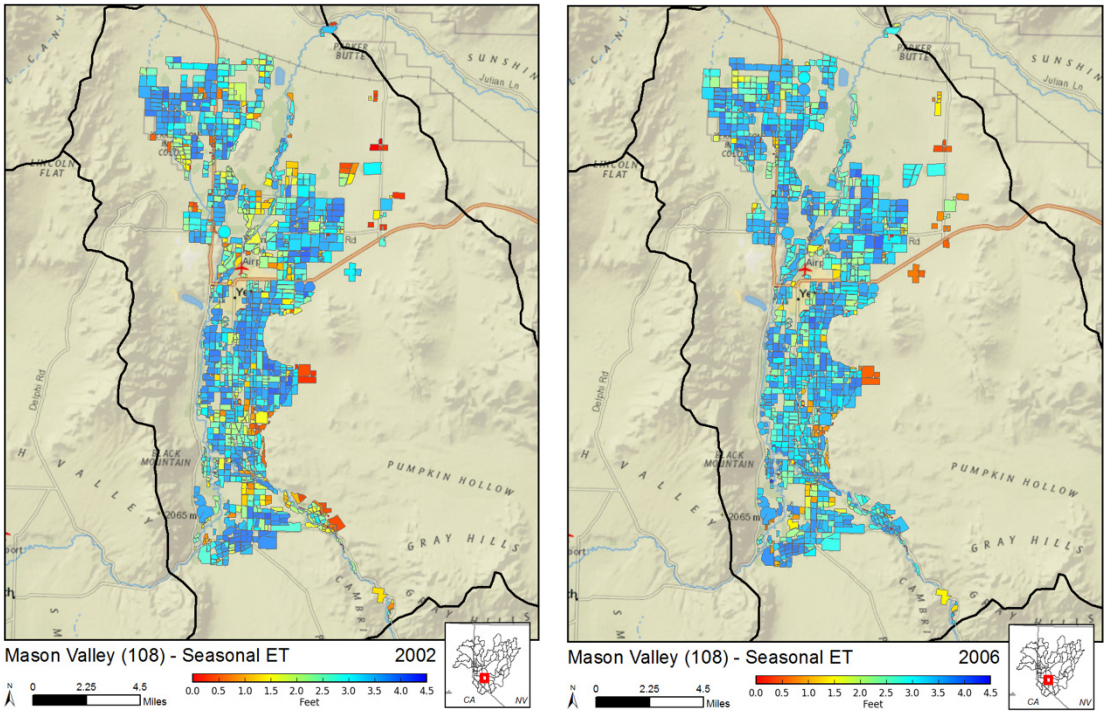


Figure 15. Spatial distribution of field average seasonal ET in Mason Valley for 2002 and 2006, dry and wet years, respectively.

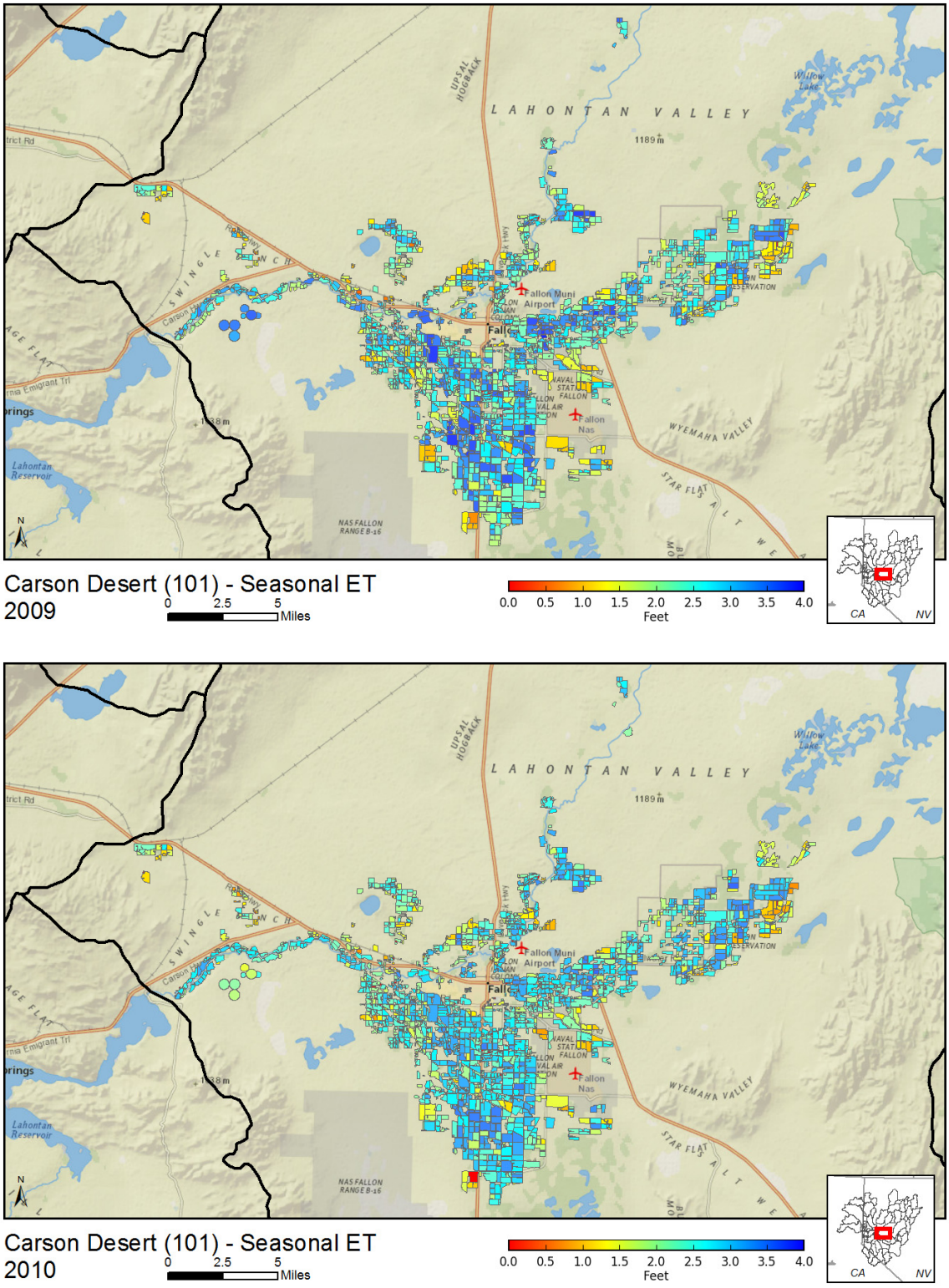


Figure 16. Spatial distribution of field average seasonal ET in Fallon for 2009 and 2010, dry and wet years, respectively

observed meteorological data, estimated weather data from METDATA, inaccuracies in Landsat radiance and reflectance, time integration of $ET_rF$ in between Landsat images, and inaccuracies in field polygon areas. However, the METRIC model applied in this study has been shown to generally be accurate to within 10 to 20 percent of measured crop ET in Nevada and other states in the western U.S. [Kalma et al., 2008; Morton et al., 2013; Serbina and Miller, 2014; Liebert et al., 2015]. For more information about limitations of the approaches applied in this study see Kalma et al. [2008], Morton et al. [2013], Huntington and Allen [2010], and Huntington et al. [2015]. These studies provide lengthy discussions about the uncertainty and limitations of remote sensing and reference ET – crop coefficient approaches for estimating crop ET.

## SUMMARY

The primary objective of this study was to develop field scale monthly, seasonal, and annual ET and net ET estimates for northwestern Nevada and northeastern California, and provide a brief discussion on the spatial and temporal variability of ET with respect to drought and land use changes. Crop ET estimates were computed from a remotely sensed land surface energy balance model, METRIC, using Landsat 5 TM and Landsat 7 ETM+ satellite imagery combined with gridded weather data estimates of ETr. Results of estimated ET, net ET, $ET_r$, and precipitation were summarized for the study period of 2001 through 2011 at monthly, seasonal (April – October), and annual time steps, and at field and basin scales depending on the variable.

Results were organized and illustrated several ways, including an ArcGIS geodatabase that contains all spatial and temporal data, map figures of field average seasonal and annual ET rates (Appendix 5), histograms of ET vs. field area per HA (Appendix 6), and annual distributions of monthly ET for each HA (Appendix 7). METRIC ET estimates compared well with previously reported ET estimates based on micrometeorological, water balance lysimetry, and soil moisture depletion techniques. METRIC ET estimates were generally well within the error of micrometeorological station derived ET estimates (~10 to 20 percent) at daily, monthly, and seasonal time steps (Figure 13; Appendix 8). METRIC ET results that represent well-watered conditions also generally compare well with $ET_r$ - crop coefficient and water balance estimates of crop ET for most HAs (Figure 14).

To assess how ET varies spatially and temporally across the study area, METRIC derived ET estimates were evaluated with respect to drought and land use changes for select HAs. Select HAs chosen to illustrate and analyze spatial and temporal ET distributions were Lovelock, Fish Springs Ranch (i.e. Honey Lake Valley), Fallon, and Mason Valley. The impact of drought was most notable in Lovelock. Fallon and Mason Valley exhibited the least amount of temporal variability in ET due to ample upstream storage and supplemental groundwater pumping, respectively. Land use change at Fish Springs Ranch was clearly evident due to a sharp reduction in ET (Figure 12).

While many previous studies have assumed that crop ET rates are temporally and spatially constant within the study area of northern Nevada, results from this study indicate that temporal and spatial distributions of crop ET are highly variable. It is recommended that spatial and temporal distributions of crop ET be considered in water budget and modeling studies for HAs where significant irrigation occurs. Landsat surface energy balance derived crop ET estimates produced in this study have many immediate applications relevant to water managers, practitioners, and researchers. Analyzing ET over long time histories and with respect to climate, crop type, water rights and availability, and land use change, is an effective way to assess historical and future impacts of drought, cumulative impacts of changing water source and crop type, and land use change. Obtaining information on historical ET and assessing this information with respect to water supply and demand will be useful for planning, adaptation, and mitigation strategies. Approaches for estimating remotely sensed crop ET, such as those outlined in this report, are now being applied by report authors in more automated and programmatic ways so that operational crop ET estimates can be easily and effectively used for water use inventories in Nevada, California, and other western U.S. states.

## ACKNOWLEDGEMENTS

This work was funded by the U.S. Bureau of Reclamation in coordination with Nevada Division of Water Resources. Funding for Landsat-based ET software development, application, and engagement with Nevada Division of Water Resources was also provided by the U.S. Geological Survey Landsat Science Team and NASA's Water Resources Applied Sciences Program. The authors thank Adam Sullivan (Nevada Division of Water Resources), Chris Garner (DRI), and Chris Pearson (DRI) for providing a detailed peer review and greatly improving the report.

## REFERENCES


Abatzoglou, J. T. (2013), Development of gridded surface meteorological data for ecological applications and modelling, Int. J. Climatol., 33(1), 121–131.

Allander, K. K., J. L. Smith, and M. J. Johnson (2009), Evapotranspiration from the Lower Walker River Basin, West-Central Nevada, Water Years 2005–07, U.S. Geological Survey Scientific Investigations Report 2009–5079, 62.

Allen, R. (2008), Quality Assessment of Weather Data and Micrometeological Flux-Impacts on Evapotranspiration Calculation, 農業気象, Journal Agric. Meteorol., 64(4), 191–204, doi:10.2480/agrmet.64.4.5.

Allen, R. G. (1996), Assessing integrity of weather data for reference evapotranspiration estimation, J. Irrig. Drain. Eng., 122(2), 97–106.

Allen, R. G. (2011), Ref-ET: Reference Evapotranspiration Calculator - Version - Windows 3.1.10. University of Idaho, Available from: http://extension.uidaho.edu/kimberly/2013/04/ref-et-reference-evapotranspiration-calculator/ (Accessed 17 April 2015)

Allen, R. G., C. E. Brockway, and J. L. Wright (1983), Weather station siting and consumptive use estimates, J. Water Resour. Plan. Manag., 109(2), 134–136.

Allen, R. G., L. S. Pereira, D. Raes, M. Smith, and others (1998), Crop evapotranspiration-Guidelines for computing crop water requirements-FAO Irrigation and drainage paper 56.

Allen, R. G., I. A. Walter, R. Elliot, and T. A. Howell (2005), ASCE-EWRI Standardization of Reference Evapotranspiration, Am. Soc. Civ. Eng. Water Inst.

Allen, R. G. et al. (2007a), Satellite-Based Energy Balance for Mapping Evapotranspiration with Internalized Calibration (METRIC)—Applications, J. Irrig. Drain. Eng., 133(4), 395–406, doi:10.1061/(ASCE)0733-9437(2007)133:4(395).

Allen, R. G., M. Tasumi, and R. Trezza (2007b), Satellite-Based Energy Balance for Mapping Evapotranspiration with Internalized Calibration (METRIC)—Model, J. Irrig. Drain. Eng., 133(4), 380–394, doi:10.1061/(ASCE)0733-9437(2007)133:4(380).

Allen, R. G., L. S. Pereira, T. a. Howell, and M. E. Jensen (2011), Evapotranspiration information reporting: I. Factors governing measurement accuracy, Agric. Water Manag., 98(6), 899–920, doi:10.1016/j.agwat.2010.12.015.

Allen, R. G., R. Trezza, M. Tasumi, and J. Kjaersgaard (2014), METRIC applications manual for Landsat satellite imagery, Version 3.0, Univ Idaho, Kimberly.

Anderson, M. C., K. A. Semmens, F. Gao, C. Hain, W. P. Kustas, J. G. Al, J. H. Prueger, L. Mckee, and W. Dulaney (2015), Monitoring Daily Evapotranspiration at Field- to-Regional Scales : An Application over California Vineyards using Landsat 8, Remote Sens. Environ., 2014–2016.

Anderson, M. C. M., R. R. G. Allen, A. Morse, and W. W. P. Kustas (2012), Use of Landsat thermal imagery in monitoring evapotranspiration and managing water resources, Remote Sens. Environ., 122, 50–65, doi:10.1016/j.rse.2011.08.025.

Bastiaanssen, W. G. M., M. Menenti, R. A. Feddes, and A. A. M. Holtslag (1998), A remote sensing surface energy balance algorithm for land (SEBAL). 1. Formulation, J. Hydrol., 212–213, 198–212, doi:10.1016/S0022-1694(98)00253-4.

Bos, M. G., R. AL Kselik, R. G. Allen, and D. Molden (2009), Water Requirements for Irrigation and the Environment, , 174, doi:10.1007/978-1-4020-8948-0.

Cammalleri, C., M. C. Anderson, and W. P. Kustas (2014), Upscaling of evapotranspiration fluxes from instantaneous to daytime scales for thermal remote sensing applications, Hydrol. Earth Syst. Sci., 18(5), 1885–1894, doi:10.5194/hess-18-1885-2014.

Carroll, R. W. H., G. Pohll, D. McGraw, C. Garner, A. Knust, D. Boyle, T. Minor, S. Bassett, and K. Pohlmann (2010), Mason Valley Groundwater Model: Linking Surface Water and Groundwater in the Walker River Basin, Nevada, JAWRA J. Am. Water Resour. Assoc., doi:10.1111/j.1752-1688.2010.00434.x.

Chander, G., and B. Markham (2003), Revised landsat-5 tm radiometric calibration procedures and postcalibration dynamic ranges, IEEE Trans. Geosci. Remote Sens., 41(11), 2674–2677, doi:10.1109/TGRS.2003.818464.

Collatz, G. J., J. T. Ball, C. Grivet, and J. A. Berry (1991), Physiological and environmental regulation of stomatal conductance, photosynthesis and transpiration: a model that includes a laminar boundary layer, Agric. For. Meteorol., 54(2–4), 107–136, doi:10.1016/0168-1923(91)90002-8.

Daly, C., W. Gibson, and G. Taylor (2002), A knowledge-based approach to the statistical mapping of climate, Clim. Res., 22(2), 99-113.

Fry, J. a. J., G. Xian, S. Jin, J. a. J. Dewitz, C. G. Homer, L. Yang, C. a. Barnes, N. D. Herold, and J. D. Wickham (2011), Completion of the 2006 national land cover database for the conterminous United States, Photogramm. Eng. Remote Sensing, 77(9), 858–864.

Gonzalez-Dugo, M. P., C. M. U. Neale, L. Mateos, W. P. Kustas, J. H. Prueger, M. C. Anderson, and F. Li (2009), A comparison of operational remote sensing-based models for estimating crop evapotranspiration, Agric. For. Meteorol., 149(11), 1843–1853, doi:10.1016/j.agrformet.2009.06.012.

Guitjens, J. C., and M. T. Goodrich (1994), Dormancy and nondormancy alfalfa yield and evapotranspiration, J. Irrig. Drain. Eng., 120(6), 1140–1146, doi:10.1061/(ASCE)0733-9437(1994)120:6(1140).

Guitjens, J. C. and C. N. Mahannah (1977), Upper Carson River Water Study, Water Year 1976. Cooperative Ext. Svc., Agric. Exp. Sta., Max C. Fleischmann College of Agric., University of Nevada, Reno, Nevada. R120. 32 p.

Halford, K. J., and R. W. Plume (2011), Potential effects of groundwater pumping on water levels, phreatophytes, and spring discharges in Spring and Snake Valleys, White Pine County, Nevada, and adjacent areas in Nevada and Utah, U.S. Geological Survey Scientific Investigations Report 2011-5032, 52 p.

Hendrickx, J. M. H. (2010), ET Mapping in the Green River Basin - Second Stage, Growing Season, Final Report to the University of Wyoming. Soil Hydrology Associates, LLC,.

Hobbins, M. T., and J. Huntington (2016), Evapotranspiration and evaporative demand. Handbook of Applied Hydrology, 2nd ed. V.P. Singh, Ed., McGraw-Hill Education, 42-1 - 42-14.

Hoffman, R. J., R. J. Hallock, T. G. Rowe, M. S. Lico, H. L. Burge, and S. P. Thompson (1990), Reconnaissance investigation of water quality, bottom sediment, and biota associated with irrigation drainage in and near Stillwater Wildlife Management Area, Churchill County, Nevada, 1986-87, U.S. Geological Survey, Water Resources Investigations Report 89 (1990): 4105.

Homer, C., J. Dewitz, J. Fry, M. Coan, N. Hossain, C. Larson, N. Herold, A. McKerrow, J. N. VanDriel, and J. Wickham (2007), Completion of the 2001 National Land Cover Database for the Conterminous United States, Photogramm. Eng. Remote Sensing, 73(4), 337–341.

Homer, C. G., J. A. Dewitz, L. Yang, S. Jin, P. Danielson, G. Xian, J. Coulston, N. D. Herold, J. D. Wickham, and K. Megown (2015), Completion of the 2011 National Land Cover Database for the conterminous United States-Representing a decade of land cover change information, Photogramm. Eng. Remote Sensing, 81(5), 345–354.

Hunsaker, D. J., J. P. J. Pinter, E. M. Barnes, and B. A. Kimball (2003), Estimating cotton evapotranspiration crop coefficients with a multispectral vegetation index, Irrig. Sci., 22(2), 95–104, doi:10.1007/s00271-003-0074-6.

Huntington, J. L., and R. G. Allen (2010), Evapotranspiration and Net Irrigation Water Requirements for Nevada, Nevada Division of Water Resources, Carson City, Nevada, 288 pp.

Huntington, J. L., S. Gangopadhyay, J. M. Spears, R. G. Allen, C. King, C. G. Morton, A. Harrison, D. McEvoy, A. Joros, and T. Pruitt (2015), West-wide climate risk assessments: Irrigation demand and reservoir evaporation projections. U.S. Bureau of Reclamation, US Department of the Interior, Bureau of Reclamation, Technical Service Center, Tech. Memo. 86-68210-2014-01, 196 pp.

Jensen, M. E., R. D. Burman, and R. G. Allen (1990), Evaporation and irrigation water requirements. ASCE Manuals and Reports on Eng. Practices No. 70. Am. Soc. Civil Eng., New York, NY, 978-0.

Kalma, J. D., T. R. McVicar, and M. F. McCabe (2008), Estimating Land Surface Evaporation: A Review of Methods Using Remotely Sensed Surface Temperature Data, Surv Geophys, 29(4–5), 421–469, doi:10.1007/s10712-008-9037-z.

Katerji, N., J. W. Van Hoorn, A. Hamdy, M. Mastrorilli, and F. Karam (1998), Salinity and drought, a comparison of their effects on the relationship between yield and evapotranspiration, Agric. Water Manag., 36(1), 45–54.

Kjaersgaard, J., and R. G. Allen (2010), Remote Sensing Technology to Produce Consumptive Water Use Maps for the Nebraska Panhandle. Final completion report submitted to the University of Nebraska, 88.

Liebert, R., J. Huntington, C. Morton, S. Sueki, and K. Acharya (2015), Reduced evapotranspiration from leaf beetle induced tamarisk defoliation in the Lower Virgin River using satellite based energy balance, Ecohydrology, doi:10.1002/eco.1623.

Lopes, T. J., and K. K. Allander (2009), Water Budgets of the Walker River Basin and Walker Lake , California and Nevada, U.S. Geological Survey Scientific Investigations Report, 5157, 44 p.

Maurer, D., and D. Berger (2006), Water Budgets and Potential Effects of Land- and Water-Use Changes for Carson Valley, Douglas County, Nevada, and Alpine County, California, U.S. Geological Survey Scientific Investigations Report, 2006-5305, 64 p.

Maurer, D. K., D. L. Berger, M. L. Tumbusche, and M. J. Johnson (2006), Rates of evapotranspiration, Recharge from Precipitation beneath selected areas of native vegetation, and streamflow gain and loss in Carson Valley, Douglas County, Nevada, and Alpine County, California, U.S. Geological Survey Scientific Investigation Report 2005-5288, 70.

McNaughton, K. G., and P. G. Jarvis (1991), Effects of spatial scale on stomatal control of transpiration, Agric. For. Meteorol., 54(2–4), 279–302, doi:10.1016/0168-1923(91)90010-N.

Mitchell, K. E. et al. (2004), The multi-institution North American Land Data Assimilation System (NLDAS): Utilizing multiple GCIP products and partners in a continental distributed hydrological modeling system, J. Geophys. Res., 109(D7), doi:10.1029/2003JD003823.

Morton, C. ., J.L. Huntington, R.G. Allen, and A. Kilic (2016), More Landsat Satellites Equates to More Reliable Monitoring of Water Consumption., Unpublished Internal Desert Research Institute Report.

Morton, C. G., J. L. Huntington, G. M. Pohll, R. G. Allen, K. C. Mcgwire, and S. D. Bassett (2013), Assessing Calibration Uncertainty and Automation for Estimating Evapotranspiration from Agricultural Areas Using METRIC, J. Am. Water Resour. Assoc., 49(3), 549–562, doi:10.1111/jawr.12054.

NRCS (2015), Description of SSURGO Database | NRCS, Descr. SSURGO Database. Available from: http://www.nrcs.usda.gov/wps/portal/nrcs/detail/soils/survey/?cid=nrcs142p2_053627

Ozdogan, M., and M. Rodell (2010), Simulating the effects of irrigation over the United States in a land surface model based on satellite-derived agricultural data, Journal of Hydrometeorology, 11(1), 171-184.

Rashedi, N. (1983), Evapotranspiration Crop Coefficients for Alfalfa at Fallon, Nevada. Thesis presented to the University of Nevada, Reno.

Rodell, M., D. Mocko, and H. K. Beaudoing (2015), LDAS: Land Data Assimilation Systems, Available from: http://ldas.gsfc.nasa.gov/index.php

Schulze, E. D., O. L. Lange, U. Buschbom, L. Kappen, and M. Evenari (1972), Stomatal responses to changes in humidity in plants growing in the desert., Planta, 108(3), 259–70, doi:10.1007/BF00384113.

Serbina, L. O., and H. M. Miller (2014), Landsat and water: case studies of the uses and benefits of landsat imagery in water resources, U.S. Geological Survey Open-File Report 2017-1034.

Snyder, D. T., J. C. Risley, and J. V. Haynes (2012), Hydrological information products for the Off-Project Water Program of the Klamath Basin Restoration Agreement, U.S. Geological Survey Open-File Report 2012-1199.

Szilagyi, J., and A. Schepers (2014), Coupled heat and vapor transport: The thermostat effect of a freely evaporating land surface, Geophys. Res. Lett., 41(2), 435–441, doi:10.1002/2013GL058979.

Tasumi, M., and R. G. Allen (2007), Satellite-based ET mapping to assess variation in ET with timing of crop development, Agric. Water Manag., 88(1), 54–62, doi:10.1016/j.agwat.2006.08.010.

Tasumi, M., R. G. Allen, R. Trezza, and J. L. Wright (2005), Satellite-based energy balance to assess within-population variance of crop coefficient curves, J. Irrig. Drain. Eng., 131(1), 94–109.

Tasumi, M., R. G. Allen, and R. Trezza (2008), At-surface reflectance and albedo from satellite for operational calculation of land surface energy balance, J. Hydrol. Eng., 13(2), 51–63.

Temesgen, B., R. G. Allen, and D. T. Jensen (1999), Adjusting temperature parameters to reflect well-watered conditions, J. Irrig. Drain. Eng., 125(1), 26–33.

Tolk, J. A., and T. A. Howell (2001), Grain Sorghum Grown with Full and Limited Irrigation in Three High Plains Soils, Trans. ASAE, 44(6), 1553–1558.

USDA Farm Service Agency (2012), Common Land Unit (CLU), U.S. Department of Agriculture.

USDA National Agricultural Statistics Service, and U.N.A.S. Service (2015), 2014 STATE AGRICULTURE OVERVIEW - Nevada, Available from: http://www.nass.usda.gov/Quick_Stats/Ag_Overview/stateOverview.php?state=NEVADA (Accessed 15 May 2015)

Vidler Water Company (2015), VIDLER | Nevada, Available from: http://www.vidlerwater.com/nevada.html

Yager, R., D. Maurer, and C. Mayers (2012), Assessing potential effects of changes in water use with a numerical groundwater flow model of Carson Valley, Douglas County, Nevada, and Alpine County, California, U.S. Geological Surevey Scientific Investigations Report 2012-5262.

Yan, L., and D. Roy (2016), Conterminous United States crop field size quantification from multi-temporal Landsat data, Remote Sens. Environ., 172, 67-86.

## APPENDICES

See https://www.dri.edu/metric-et for digital files of appendices.

# STANDING DISTRIBUTION LIST

*****Nevada State Library and Archives
State Publications
100 North Stewart Street
Carson City, NV 89701-4285

Archives Getchell Library
University of Nevada, Reno
1664 N. Virginia St.
Reno, NV 89557
tradniecki@unr.edu

Document Section, Library
University of Nevada, Las Vegas
4505 Maryland Parkway
Las Vegas, NV 89154
sue.wainscott@unlv.edu

†Library
Southern Nevada Science Center
Desert Research Institute
755 E. Flamingo Road
Las Vegas, NV 89119-7363

***All on distribution list receive one copy, unless otherwise noted.***

---

***** 12 copies
† 3 copies; CD with pdf (from which to print)